ELLIPTIC FLOW IN HEAVY ION NUCLEAR REACTIONS

Thesis submitted in partial fulfillment of the requirement for
The award of the degree of
Masters of Science
In
PHYSICS

Submitted by

Kirandeep Kaur
Roll no. - 30704007

Under
the guidance of
Dr. Suneel Kumar

School of physics and Material Science
Thapar University
Patiala – 147004 (PUNJAB)
INDIA

CERTIFICATE

This is to certify that Ms. Kirandeep Kaur, Roll No. 30704007 has worked on this thesis report as a partial fulfillment for award of the degree of MASTERS OF SCIENCE in physics. I certify that the matter embodied in this report is of candidate's own record and not submitted to any other university in any part or full form for the award of such a degree.

S Kumar

(Dr. Suneel Kumar)
Supervisor
SPMS, Thapar University
Patiala

Countersigned by:

Dr. O.P.Pandey
(Prof. & Head)
School of Physics and Materials Science
Thapar University, Patiala.

Dr. R.K. Sharma
Dean of academic Affairs
Thapar University
Patiala.

ACKNOWLEDGEMENT

Knowledge in itself is a continuous process. I would have never succeeded in completing my task without cooperation, encouragement and help provided to me by various personalities.

My foremost thanks goes to my to worthy superviser **Dr. Suneel Kumar**. Without him, this dissertation would not have been possible. I thank him for his patience and encouragement that carried me on through difficult times, and for his insights and suggestions that helped to shape my research skills. I express my sincere thanks to him for his valuable guidance in carrying out work under his effective supervision, encouragement and cooperation. His visionary thoughts have influenced me greatly.

I also thank **Dr. O. P. Pandey**, Professor and Head, School of Physics and Material Science for his support and providing facilities.

I wish to express my thanks to **Mrs. Varinderjit Kaur** and **Mr. Sanjeev Kumar**, Research Scholars for the help and valuable suggestions whenever I needed out of their busy schedule.

All my friends and the staff at the School of Physics and Material Sciences are acknowledged for providing me a friendly atmosphere and encouraging me throughout this work. Their assistance and partnership were of great pleasure. Their views were very insightful and helpful. I am deeply thankful to my Family, their moral support and patience has bared fruit through completion of this Thesis which will result in award of the prestigious degree of M.Sc.

Above all I render my gratitude to the Almighty who bestowed self – confidence, ability, strength and path to me in accomplishing this work.

Kirandeep Kaur

KIRANDEEP KAUR

ROLL NO. 30704007

ABSTRACT

Elliptic flow develops because of almond shape of the overlapping region in a heavy ion collision. Elliptical or higher order azimuthal shapes can provide help (a) when the phase space coverage is limited to a narrow region around midrapidity, and (b) at beam energies close to the balance energy, where no net deflection of nucleons is observed. The elliptic flow is expected to be larger in more peripheral collisions because of the anisotropy in coordinate space which is the source of this flow. The study of elliptic flow provides valuable data on the nuclear equation of state and isospin dependent N-N cross section. Study of dependence of elliptic flow and different fragment flows on beam energies, mass number, isospin and impact parameter have revealed quite interesting physics about the properties and origin of collective flow.

TABLE OF CONTENTS

LIST OF FIGURES

CHAPTER – 1

INTRODUCTION

1.1 Heavy ion collisions in the nucleonic regime

The last decades have seen an accumulation of an impressive corpus of nuclear properties close to equilibrium. What picture do the heavy-ion collisions present scenario display? The answer is that the study of heavy ion-collisions in the nucleonic regime is twofold. There is, first, an interest in understanding the time evolution of the reaction starting from a highly-out-of-equilibrium situation (two cold colliding nuclei) towards a possible thermalized system by means of dissipation. Second, reaction products are in extreme states in the sense that they can be highly exotic or hot. Exotic nuclei have unusual neutron/proton ratio or a very large number of neutrons (super heavy elements). Hot nuclei have excitation energies close or even higher than their total binding energies. Studies of nuclei at finite temperatures are incomplete without an explicit account of the dynamics.

Heavy ion collisions (HIC) at intermediate and high energies provide a possibility for studying the properties of nuclear matter in conditions vastly different than in normal nuclei, such as high density, high temperature and excitation as well as large difference in the proton and neutron numbers [1-3]. The nuclear equation of state (EOS) can be researched via liquid–gas transition, multi-fragmentation and collective flow, such as directed and elliptic flow produced in heavy ion collisions. Such knowledge is of interest in nuclear physics. Heavy ion collisions are useful in understanding astrophysical phenomena such as the properties of the core of compact stars, the evolution of the early universe, and the formation of elements in stellar nucleosynthesis.

One observable that has been extensively used for extracting such information from heavy ion collisions is the collective flow of various particles. For example, the proton flow in heavy ion collisions at 200 MeV/nucleon to 1 GeV/nucleon has been found to be consistent with a soft nuclear equation of state [4-5].

1.2 Heavy ion nuclear reactions

Nuclear matter consists of an equal and infinite number of nucleons and protons distributed uniformly throughout space, but with the neglect of Coulomb forces. At low densities, nuclear matter is unbound because nuclear forces are only felt at short range. It is possible to explore the nuclear equation of state, related to dependence of energy on density and temperature. This equation is essential for understanding of star formation and development. A typical plot of the energy dependence on density is shown in fig 1 for nuclear matter.

A minimum energy corresponds to the volume energy of equation $E_v = +a_v A$, about -15.6 MeV. The curvature at the minimum, $\frac{d^2E}{d\rho^2}$, is related to compressibility of nuclear matter,

$$K = 9\left(\rho^2 \frac{\delta^2 E}{\delta \rho^2}\right)_{min}$$

The value of K is about 200MeV. The rapidity of the rise of E with increasing density is a matter of debate, and it has been conjectured that metastable forms of nuclear matter may exist, as shown by long dashed curve in fig 1.1.

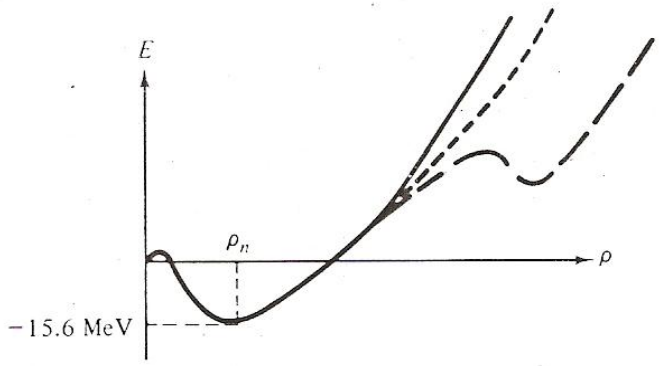

Figure1.1: Energy of nuclear matter as a function of density at a temperature of 0K. The steepness of the curve in high energy region is not known well, as shown by the solid and short dashed lines, and a second minimum , shown by the long dashed curve could occur.

The series of drawings in fig 1.2, show typical events in heavy ion reactions with increasing energy. The dynamics are determined by the competition between the Coulomb force, the centrifugal barrier, and the nuclear force. Owing to these forces, the shapes of the nuclei change as they approach each other and surface modes of motion are excited. For energies below the Coulomb barrier, the Coulomb excitation dominates the interaction. Above the Coulomb barrier, many nuclear processes occur. Examples are particle transfers, fusion reactions, and nuclear excitations, often with large angular momenta, particularly for grazing collisions. To see that very high angular momenta can be reached and to study the collisions in more detail, we note the semi-classical approach can be used because $\frac{pr_c}{\hbar} >> 1$, where p is the relative momentum of the two colliding ions and r_c is the approximate distance of closest approach . For energies close to the Coulomb barrier, this distance can be found by assuming that the nuclei remains undistorted. In that case, the classical distance of closest approach is given approximately by:

$$r_c \approx \frac{Z_1 Z_2 e^2}{E_K} ,$$

where Z_i is the atomic distance of ion I and E_K is the relative kinetic (c.m.)energy.

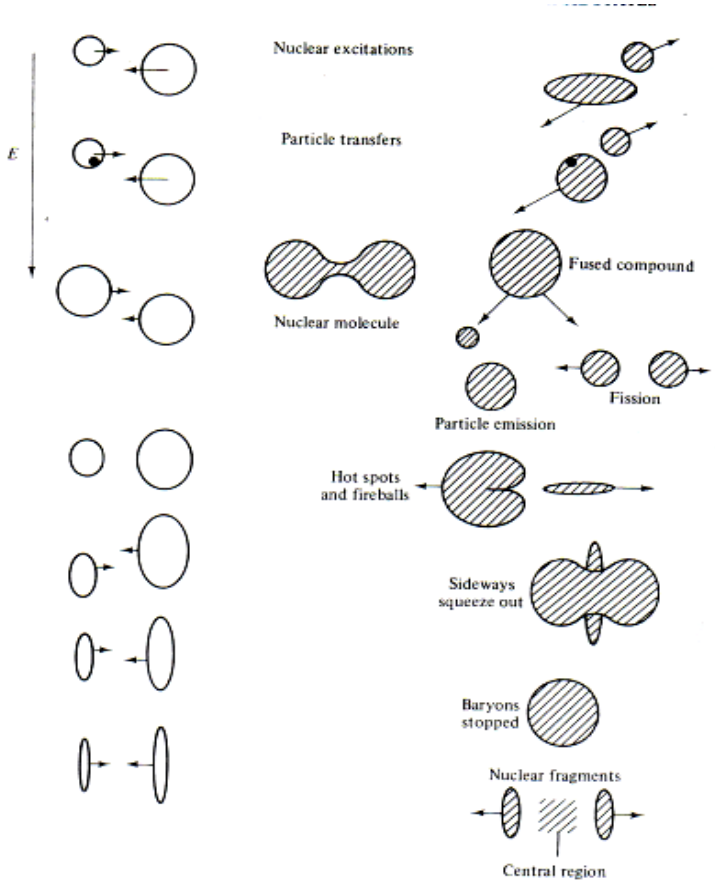

Figure 1.2: Sketches of some heavy ion reactions as a function of increasing energy.

Consider ^{16}O ions of 150 MeV bombarding ^{199}Hg. The centre of mass energy is somewhat larger than 139 MeV, and the distance of closest approach about 6.8 Fermi. The parameter $\frac{pr_c}{K}$ =82 is much larger than 1, as required by the semi-classical approximation. Angular momenta up to this magnitude can be excited, particularly if the nuclei fuse together, since the approximate height of the Coulomb barrier,

$$\frac{Z_1 Z_2 e^2}{R_1 + R_2} \approx 90 \text{ MeV}, \text{ with } R = R_0 A^{1/3}$$

Fusion reactions are also likely to occur in central collisions. The Coulomb barrier slows down the nuclei so that fusion is more probable. If the nuclei fuse, then a "compound nucleus" is formed that can be heavier than known stable nuclei. It may de excite in many ways, including fragmentation into several pieces or fission into two fragments.

As the collision energy increases, the number of possible reaction products grows rapidly and the reaction becomes more complex; the production of pions and other mesons increases its importance. The nucleus can be treated as a quantum fluid. When the velocity of the projectile is much larger than the average speed of the nucleons in the nucleus , then these nucleons cannot move aside to accommodate the projectile; this leads to a high density and the disorganisation leads to heating. Head-on collisions may produce shock waves if the mean free path of the nucleons is much smaller than the nuclear-radii; but no direct evidence exists. Particularly in off centre collisions, nuclear material may be squeezed out sideways as shown in fig 1.2.

Classification of heavy-ion reactions by energy E:

E < 10 MeV/A:	low – energy heavy ion reactions,
10 MeV/A <E <100MeV/A:	heavy-ion reactions at medium energies,
100 MeV/A <E < 10 GeV/A:	relativistic heavy- ion reactions,
E>10GeV/A:	ultra-relativistic- heavy ion reactions.

Features particular to heavy ion reactions:

- Because the incident particle often has a mass comparable to that of the target, a large fraction of the kinetic energy goes into centre of mass motion.

- Both reaction partners have a high charge, hence Coulumb forces become significant and many phenomenon result from interplay of Coulumb and nuclear forces.

- In the interaction region, intermediate states with as many as 300 to 400 nucleons are formed. Therefore, in the description of the system, macroscopic aspects must be taken into account to a larger extent than in light-body induced reactions.

- In the peripheral collisions, the nucleus–nucleus interaction proceeds via partial waves corresponding a large orbital angular momentum of relative motion ($L \geq 100\hbar$).

- The de-Broglie wavelength of relative motion is small compared with the characteristic geometric dimensions of the system, so that the relative motion may be treated by classical considerations using collision parameters and trajectories.

- In heavy ion reactions , nuclear states with very high spins can be excited.

- In the reaction $Ca_{20}^{40} \longrightarrow Pb_{82}^{208}$, an orbital angular momentum of about $140\hbar$ may be reached at the Coulomb barrier . Such high angular momenta allow the production of superdeformed nuclei with cigar like shapes.

- For Ca_{20}^{40}-ions with an energy of 10 MeV per nucleon. The De Broglie wavelength is λ = 0.5 fm.

The figure 1.3 shows the diagram of heavy ion collision. In this figure two nuclei are shown approaching each other with certain impact parameter. It is a non central collision. The nucleons which participate in the collision are the participants and the nucleons which donot undergo any collision are called the spectators.

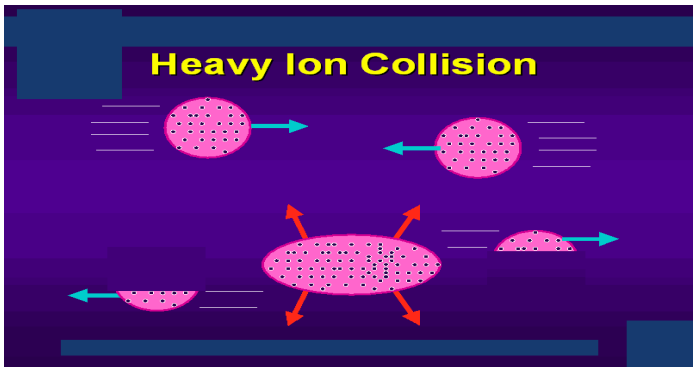

Figure 1.3: Heavy ion collision

1.3 The nuclear phase diagram

The phase diagram of nuclear matter gathers in the density-temperature plane the various observed or predicted phases of nuclear matter. All nuclei possess a common central density known as density of saturation, denoted by $\rho_0 \approx 0.17\ fm^{-3}$. The point of density ρ_0 and zero temperature is known as the saturation point of nuclear matter. High densities/temperatures may be obtained only by strongly perturbing nuclei. This occurs naturally in the cores of type II supernova where nuclei may be heated up to temperatures of order 10 MeV, which is sufficient to sensibly affect the structure of nuclei. On the other hand, supernovae cores are not extremely dense, their density being only of order ρ_0. Neutron stars, in contrast, involve very high densities(typically two or three times ρ_0) but temperatures virtually vanish, from a nuclear physics point of view, in these objects($T \approx 10^6 K \approx 10^{-4} MeV$).

At moderate temperatures, the structure of the nucleon-nucleon interaction suggests properties similar to real Vander Waals fluids. At very high temperature/density ($\rho \approx 10-20\rho_0$ and/or T ≈ 150-200MeV) one expects a transition of nuclear matter to a quark

gluon plasma (QGP). At such high energies quarks and gluons, usually bound in nucleons and/or mesons and baryons, become deconfined. QCD calculations provide estimates of deconfinement for energy densities of the order of a few GeV per fm^3, which is comparable to the nucleon mass. This deconfined phase should have excited during the very first instants of the universe, according to the big bang model. Below the transition region towards the QGP one also encounters 'exotic' phases appearing as mixtures of nucleons and mesons and/or internal excitations of nucleons. The latter regions of the phase diagram are often referred to as regions of pionic or hadronic matter.

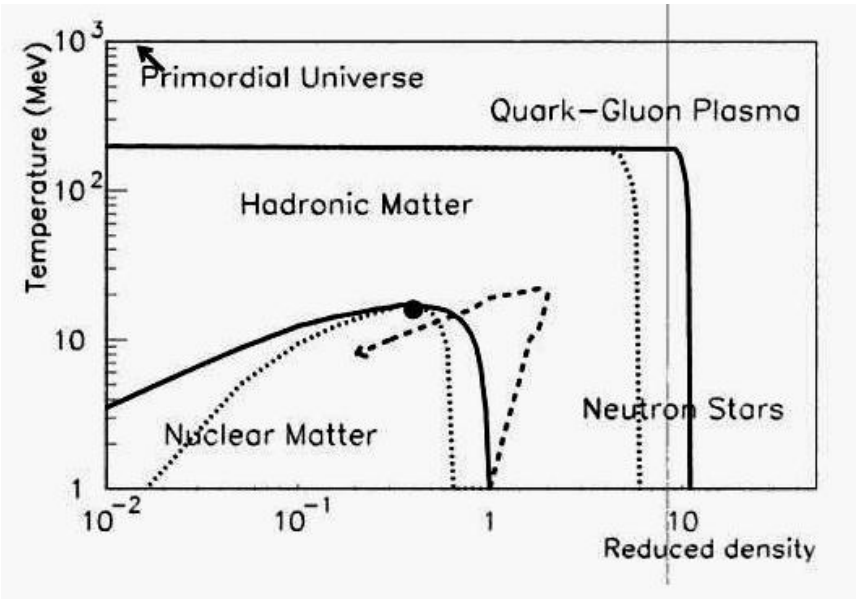

Figure 1.4**:** phase diagram for nuclei

Figure 1.4 shows the phase diagram (density (in units of saturation density) versus temperature (in MeV)) of nuclear matter. The core of nuclei in their ground states corresponds to T=0MeV and ρ/ρ_0=1. The boundary of the predicted QGP is indicated by the full line at high T(the broken line corresponds to the limit of the predicted coexistence region with hadrons). Very high temperature and densities are presumably the physical conditions which prevailed in the primordial universe. Neutron stars correspond to a dense ($\approx$3 times saturation density) and cold phase. Temperatures between 20 and 200 MeV

correspond to a region in which all hadrons are present: this is called hadronic matter. At low temperatures, only nucleons in their ground state are present. They can be ‘confined’ in drops of matter: this is the nuclear matter region. Due to the structure of the nucleon-nucleon interaction, the coexistence of a liquid and a gas phase is predicted. The full line in this region is the coexistence curve while the black point is the critical point. The region between full and broken lines is the metastable region. One expects to be able to explore large regions of the phase diagram through heavy-ion collisions, with varying beam energies (a schematic trajectory as indicated in the figure). In this case the collision must be described in a dynamical framework, namely as a path in the phase diagram.

1.4 How to explore the nuclear matter phase diagram

What do we know about nuclear matter? A direct access to supernavae cores or neutron star matter is impossible. Furthermore, the physics of these objects is by no means a purely nuclear problem: access to the nuclear aspects is complicated by astrophysical questions. On earth, it is the central part of heavy nuclei which constitutes the best access to nuclear matter. But ground-state nuclei allow at best an exploration of the close vicinity of the saturation point. Here again difficulities show up. First one should keep in mind the intrinsic limitation due to finiteness of nuclei which typically contain less than 250 nucleons, because of Coulombic effects. To extract the universal properties of infinite nuclear matter from such finite systems is thus by no means simple. Another difficulty lies in the fact that ground-state nuclei naturally provide very little information on nuclear matter. In order to explore large regions of the nuclear matter phase diagram one needs to perturb nuclei significantly, which will add an extra complication to extracting the nuclear matter properties themselves.

Heavy ion collisions turn out to constitute the best tool for investigating the properties of nuclear matter in large regions of phase diagram. In the course of the collision matter is compressed and heated up. Depending on initial conditions, various densities and temperatures can be reached and thus a large scale exploration of the nuclear matter phase diagram is possible. For example, the transition from hadronic matter to QGP is actively

sought in today's experiments with ultra-relativistic heavy ions, at beam energies of several tens of GeV per nucleon.

Heavy-ion collisions hence seem to offer a unique opportunity for exploring the phase diagram of nuclear matter. However, one has to pay a heavy tribute for this possibility; namely the fact that this exploration is no longer static but dynamical. Heavy ion collisions thus appear as paths rather than points in the phase diagram of nuclear matter. A typical heavy ion collision lasts at most a few 10^{-20} sec, often hardly long enough to allow a proper definition of the notion of temperature in such a system. The exploration of the nuclear phase diagram can hence only be understood in a non-equilibrium context, which outlines the limitations of such studies. One has to remain cautious in the interpretation of nuclear collisions in the context of the nuclear phase diagram, because it makes sense only as long as the thermodynamical variables such as temperature are properly defined. Furthermore, understanding the underlying physics and linking it to nuclear matter equation of state requires the development of specific dynamical approaches. This makes the problem more complicated, but it should also be noted that it makes it richer. Heavy-ion collisions are thus not to be considered only as a tool for investigating the nuclear matter phase diagram. They also lead to far-from-equilibrium dynamical situations in finite quantum systems. Their understanding requires original techniques which may find valuable applications in several fields of physics.

1.5 Experimental scenario

The first experiment at Berkley served mainly to get the experimentalists and theorecians aware of the problems and pitfalls of the way from medium energy heavy ion collisions to the equation of state. Later on several accelerators were built at Michigan state university (USA), GANIL (France), and at GSI (Germany). The SIS (heavy ion synchrotron) accelerator at GSI is specifically designed to study the heavy ion collisions at intermediate energies. The MSU group at Michigan state university is very active in studying fragment's spectra at lower side of the bombarding energies. The similar effort are also made by the

INDRA group at GANIL. The ALLADIN group at GSI has gone ahead and provided a complete spectra of the fragments. These measurements include the incident energies upto 1A GeV.

The INDRA collaboration at GANIL is studying mainly the collisions where large multiplicities of the nucleons are observed in the exit channel. They have undertaken a wide program where influence of different parameters on multi-fragmentation is studied. In particular, the size effects are studied in symmetric collisions of ^{36}Ar +KCl (at 32A, 40A, 52A and 74A MeV)[6], $^{58}Ni+^{58}Ni$ (at 32A,40A,52A,63A,74A,82A and 90A MeV)[6] ,$^{129}Xe+^{118}Sn$(at 25A,32A,40A,45A and 50A MeV)[7],$^{181}Ta+^{197}Au$(at 33A,39A MeV) and $^{238}U+^{238}U$ (at 24A MeV)[6]. Naturally, for studying the gentle compression and Coulumb instabilities, they have to go to heavy fragments. The collision of light systems leads to the vapourization. Recently, a detailed theoretical study of INDRA experimental findings was carried out by Aichelin and coworkers[8].

The Berkley group has concentrated mainly on the asymmetric reactions like $^{197}Au+^{197}Au$, ^{51}V , and ^{64}Cu at 60A MeV [9] or $^{36}Ar+^{197}Au$ at 50A and 110 AMeV[10] , $^{56}Fe+^{197}Au$ at 50A and 110A MeV [11] ,$^{139}La+^{12}C$ at 50A, 80A and 100A MeV[12], and $^{139}La+^{12}C$, ^{27}Al, ^{40}Ca , ^{64}Cu , ^{139}La at 35A, 40A, 45A and 55A MeV [12]. They concentrated on different probabilities which include the excitation energy, the angular distribution and the velocity distribution etc. Another symmetric reactions studied were carried out using AMPHORA detector at SARA (France)[14].

The FOPI and ALADIN groups at GSI are studying the variety of reactions giving nearly all kinds of possibilities. It ranges from ^{12}C to ^{208}Pb and with incident energy between 100A and 1000A MeV [15-22]. A lot of physical conclusions are also drawn from these studies.

Therefore, in the past years a very active program has developed at many places. SIS at GSI has replaced Bevalac as the main accelerator in what is now called intermediate

energy ($\approx$ 100 MeV upto 2 GeV per nucleon). This facility has made a big impact with three new second generation experiments, FOPI, ALADIN and KAOS. At lower energies MSU and GANIL complement the program.

There are many research groups working on IQMD model at international level which include Centre of Theoretical Nuclear Physics, National Laboratory of Heavy Ion Accelerator, Lanzhou (China), CCAST (World Laboratory), Beijing and Lawrence Berkely National Laboratory, University of California[23,24].

At present, several experimental groups are engaged in extracting information of nuclear EOS from multifragmentation and nuclear flow/fragment flow. Many body nuclear dynamics group at INDIANA University Bloomington, USA studied the role of nuclear equation of state (EOS) in particular how the density dependence of the symmetry energy affects the properties of nuclear matter[25]. TAPS collaboration studied the role of nuclear incompressibility in the production of hard photons in heavy ion collisions[26].

Recently E802 collaboration studied mid rapidity energy distribution[27]. Moreover NA49 collaboration has recently performed a series of measurements of ${}^{208}_{82}Pb+{}^{208}_{82}Pb$ collisions at 20, 30, 40, 80 and 158 MeV/A [28].

1.6 Multifragmentation

Heavy-ion collisions offer the possibility to probe nuclear matter under different conditions of densities and temperatures. At high excitation energies the nuclei may break-up into many intermediate-mass fragments, the so called multifragmentation. In multifragmentation, nuclear matter at low densities and, more generally, modes of disintegration of dynamically unstable systems are probed. In particular, the expected link with the nuclear liquid-gas phase transition provides a continuing motivation for studying multifragmentation. In these reactions, systems of small and intermediate-mass nuclei surrounded by a nucleon gas may be produced, with properties close to what is expected in

stellar processes as, e.g., supernova II explosions. Experimental extraction of in-medium modifications of the properties of hot nuclei, in particular, their symmetry energy will be important for understanding the production of nuclei and their interaction in stellar matter. Also properties of the high-density zones of the collision may be studied in the fragmentation of excited projectile spectators. The velocities of projectile residues are predicted to be sensitive to the non-local features of the nuclear mean field. Nuclear multifragmentation process, is schematically illustrated in figure 1.5 below which shows the break-up of an excited nucleus into several fragments.

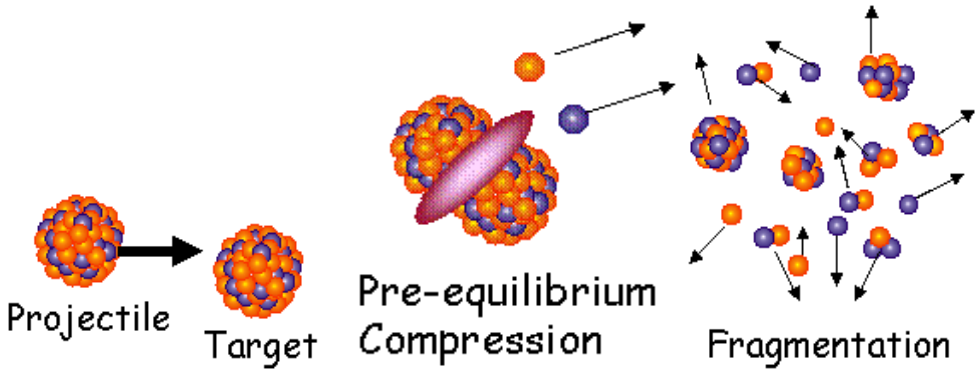

Figure 1.5: Multifragmentation in non central collisions

The study of reaction mechanisms in heavy-ion collisions between 20 and 100 MeV/nucleon is inextricably linked to that of multi-fragment emission or multifragmentation. At these energies, most reactions lead to the copious production of intermediate masss fragments (IMF) with atomic numbers $Z \geq 3$ [29]. Especially the ALADIN experiment has established the systematics of multifragmentation as a function of mass and energy[30]. The data have been used to test macroscopic models that have been combined with statistical multifragmentation models [31].

Dynamical effects in these collisions play an important role where there is strong competition between the nuclear mean field and nucleon-nucleon collisions. Experimental evidence for such effects includes:

- preequilibrium emissions
- light particle and IMF production at mid-rapidity
- determination of evaporated and non-evaporated particles
- non-spherical multifragmenting sources in central collisions

All new possibilities and ideas make multifragmentation as one of the most interesting subjects with the potential to determine the nuclear equation of state at densities below ground state density and to study phase transition in small systems. Such studies could lead to tools and methods that can be applied in the search for Quark-Gluon plasma and in other areas of physics.

1.7 Flow

When two nuclei approach each other, they feel attractive potential causing the collective transverse momentum in the direction opposite to the impact parameter. As soon as colliding nuclei overlap, particles with very large momenta are positioned closely in the configuration space due to which the potential becomes repulsive and accelerates the particles in the transverse direction . Whereas outside the overlap zone, there are either projectile or target nucleons, and therefore, the potential is still attractive. As a result of this, there is a strong potential gradient perpendicular to the beam direction in the reaction plane (where reaction plane is defined by the impact parameter b and the beam axis z) due to which an appreciable amount of the transverse momentum is transferred to the detected particles along the direction of impact parameter. This transverse momentum causes the system to expand radially, thus decreasing the density. A pictorial display of in-plane bounce off and squeeze out is presented in Fig. 1.6.

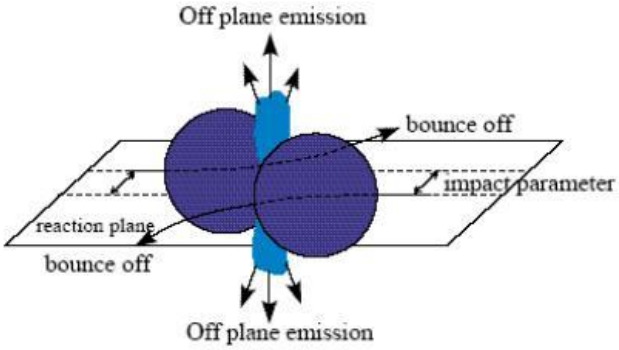

Figure 1.6 : Display of the in-plane bounce off caused by compression, and the squeeze out, the enhanced emission of light particles perpendicular to the plane close to midrapidity.

If two nuclei collide and a high density zone is built up the potential interactions of the compressed zone may become rather strong and initiate collective effects. Two major effects can be found which have been (qualitatively) predicted by hydrodynamical calculations and have been confirmed by experiments:

1. A deflection of the projectile and target remnants (which do not belong to the overlap region of the two nuclei and thus are called spectators) by the high density region (the so-called participants). These particles get a sideward kick which is called the bounce-off.

2. Particles of the high density region escape from the compressed zone. They are squeezed-out perpendicular to the reaction plane, i.e. in that direction where no remnants of the nuclei are covering the compression region.

Flow is caused by the short range nuclear repulsion and its strength decreases with decreasing energy. At very low energy the attractive part of the nuclear potential becomes more important and the direction of flow is reversed. This disappearance of flow can be observed experimentally [32]. The energy at which flow is zero is called balance energy. It can be determined very precisely and is quite independent of detector biases. Detailed and systematic measurements of the balance energy as a function of mass have been performed. Fig 6 shows a summary of these studies [33] and a comparison with BUU calculations. One

can also infer from fig 1.7 that the balance energy does not depend strongly on equation of state. This is not astonishing, given the low density at those energies, but the effect is expected to depend strongly on the in-medium cross sections.

The detailed study of flow has been considered the best way to pin down some of the parameters of the nuclear equation of state. As a consequence systematic measurement have been performed in many experiments at many accelerators. Another sign of progress is that systematic comparisons with different models (like IBUU, QMD, IQMD) now are being done in routine.

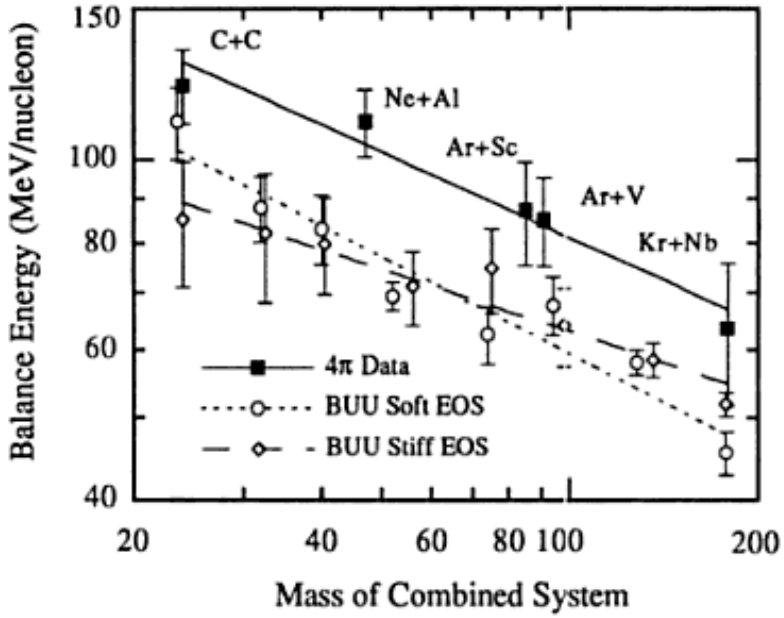

Figure 1.7: The balance energy as a function of the mass of the combined system is compared with BUU calculations with soft and stiff equation of state[33].

Composite particles show larger flow effects. In a thermal picture, the mean kinetic energy of all particles is the same, which means that the mean energy per nucleon decreases with increasing mass. The collective boost from flow, however is independent of fragment mass and therefore becomes more important with increasing mass. The FOPI collaboration has emphasized the importance of the fragments in their systematic analysis of directed fragment flow and the new evidence for "radial" flow.

Nuclear collective flow is a kind of collective phenomena found in intermediate and high energy heavy ion collisions. Study of dependence of directed flow, elliptic flow and different fragment flows on beam energies, mass number, isospin and impact parameter have revealed quite interesting physics about the properties and origin of collective flow.

Elliptic flow develops because of the almond shape of the overlapping region in a heavy ion collision. The elliptic flow is expected to be larger in peripheral collisions because of the anisotropy in coordinate space which is the source of this flow. The study of directed and elliptic flow provides valuable data on the nuclear equation of state and isospin dependent N-N cross section.

The figure below shows the diagram of radial flow, elliptic flow and directed flow.

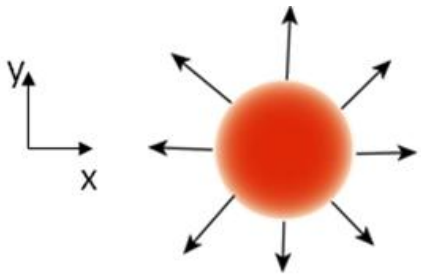

- Only one type of transverse flow in central collision (b = 0) is radial flow. (Integrates pressure history over complete expansion phase).

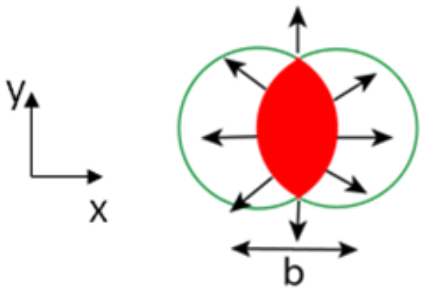

- Elliptic flow (v_2), hexadecupole flow (v_4), v_6,…caused by anisotropic initial overlap region (b>0). (More weight towards early stage of expansion)

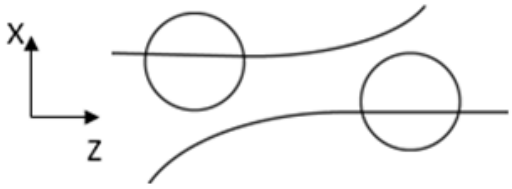

- Directed flow (v_1), sensitive to earliest collision stage (b>0). (Pre-equilibrium at forward rapidity, at midrapidity perhaps different origin.

1.8 Theoretical methods

As two heavy nuclei approach each other in a collision, they form a highly-correlated strongly-interacting finite quantum system. As they collide and the beam energy is distributed, the participant nucleons reach higher energy levels where the Pauli principle is less restrictive on the energy transfer. At this point the nuclear Fermi-gas begins to resemble a more classical one, and thus one is allowed to speak of temperature and phase transitions in the classical sense. After presumed phase transition takes place, the system expands and disassembles into clusters (liquid droplets and gaseous particles), which continue de-exciting by further fission and photon particle emission.

This transition from a quantum regime to a more classical one, and back again to the quantum world, makes heavy-ion reactions practically impossible to track analytically. Apart from being a many-body system (for which no exact solutions exist), the reaction dynamics are highly out-of-equilibrium and required the use of quantum kinetic theory which does not exist yet. Fortunately, since the collision can be divided into, say, three stages, collision/compression, expansion/breakup, and cooling, computational models with some predictive power have been devised.

Theoretically, several models have been developed which make the situation more complicated. The key point to remember is that heavy-ion collision involves very complicated non-equilibrium physics, therefore, its numerical modelling is not straight forward. Due to lack of free space at low incident energies about 98% of the attempted collisions are blocked. The whole dynamics at low energies is governed by the mean field or by the two body and three body interactions. In contrary the availability of large free phase space at relativistic energies (>2 GeV) makes Pauli principle's role quite small (roughly 4% collisions are blocked) and hence the dynamics of reaction is governed by the Cascade picture. On the other hand, both Cascade and mean field emerges at intermediate energies.

These models can be broadly divided into dynamical and statistical models, with some hybrid approaches linking these two extremes.

TDHF: The conventional theories like time dependent Hartree-Fock (TDHF) [34-36] or its semi-classical version the so called Vlasov equation (in phase-space) are suitable approaches at low energies where the nucleon-nucleon collisions are negligible. A suitable (and reasonable) approach for intermediate energy heavy-ion physics should treat the nucleon nucleon collisions and mean field on equal footing. Some attempts were made in the literature to extend the TDHF to take care of the residual nucleon-nucleon (NN) interactions which are responsible for two body collisions (this was dubbed as ETDHF)[37]. However due to complications, this theory could not be used for large scale investigations.

Boltzmannn-Uehling-Uhlenbeck: Increasing in complexity from a single-particle description mean fields can be introduced to modulate the overall behaivior of nucleons. In the BUU model, the heavy ion collision is described by the temporal evolution of the one-body density within mean field. This mean field is usually taken as that produced by the motion of the nucleons averaged over an ensemble of configurations.

Other related approaches are the Vlasov-Uhenling-Uhlenbeck and the Boltzmann-Langevin methods. The two body collisions are treated in a rather phenomenological way by employing the Monte-Carlo technique. As all these techniques use only a mean field ignoring higher order correlations, these approaches, along with BUU, are not able to explore cluster formation. Refined models introduce mean field fluctuations to artificially induce clustering, or are used in hybrid models to add an ad hoc fragmentation.

Molecular dynamics: The classical molecular dynamics (MD) [38-40] approach is capable of treating both compression and fragment formation. The molecular dynamics predicts the collective flow in a qualitative agreement with the data. It incorporates the complete classical N-body dynamics which is necessary to describe the formation of fragments. Naturally, the simple classical molecular dynamics needs refinement which should also include quantum features. In nuclear physics, the key problem in MD methods lies in the treatment of the Pauli principle. Nucleons are fermions and it is difficult to speak of nuclei without the Pauli principle. This question is simply overlooked in strictly classical calculations. MD methods with Pauli principle address this question but with disputable success.

Quantum Molecular Dynamics: The QMD model [41,42]attempts to manipulate a many-body wave function to introduce the correlations needed for cluster formation. Taking the wave function as a product of coherent states and using momentum dependent interactions with Pauli blocking, the model evolves a set of test particles through the temporal evolution of the reaction.

In past decade, several refinements and improvements were made over original QMD.

The QMD model takes into account the Pauli principle, but through two-body collisions, which is somewhat contrary to MD picture. In view of the difficulties encountered with taking the Pauli principle in classical MD methods properly into account, a new class of approaches was developed in the beginning of the 1990s, the so called fermionic molecular dynamics:FMD for fermionic molecular dynamics[43,44] and AMD for antisymmerized molecular dynamics[45,46]. The serious numerical problems have restricted the use of FMD and AMD approaches to light nuclei

These new versions were named as IQMD (Isospin-QMD), GQMD(G-matrix-QMD)[45,46]. It is worth to mention that the Intra nuclear Cascade model (INC) developed by Cugnon *et al*[47], is one of the pioneering models in the field and has acted as a guideline for the development of the field.

Isospin dependent Quantum Molecular Dynamics: IQMD model[48,49] in heavy ion collisions is used for studying the isospin effects on nuclear transverse collective flow, on nuclear radial flow and nuclear fragmentation.

The dynamics in the formation of the transient state is mainly governed by three components, namely, the mean field, two body collisions, and Pauli blocking. For an isospin dependent reaction dynamics algorithm it is essential that all the three components should reasonably include isospin degrees of freedom. In addition, it is also important that, in initialization of projectile and target nuclei, the samples of neutrons and protons in phase space should be treated separately since there exists a large difference between neutron and proton density distributions for nuclei. IQMD model is developed just on above basis. It has been shown that the IQMD can be used with large success for studying the effects of isospin in heavy ion collisions at intermediate energies.

1.9 Cluster analysis:

The minimum spanning tree method (MST) [50-52] is used in cluster analysis and track finding, if we consider tracks to be clusters of points. This method identifies two

nucleons in a same fragment if their centroids are less than a distance d_{min}. Before one can study the origin of fragments one has to identify the fragments.

$$| r_i - r_j | \leq d_{\min}$$

where r_i and r_j are the special positions of both nucleons.

One simulates the reaction using QMD. Then spatial distance of all nucleons is checked. A nucleon is part of a fragment if there is another one within a distance of $r_{\min}$=4 fm. Recently a new approach has been developed which defines the fragments in phase space. There nucleons can form fragment if the total energy/nucleon is below a minimum binding energy. Till today, this method is one of the most extensively used methods.

1.10 References:

[1] W.Cassing, V.Metag, U. Mosel and K.Naiita ,Phys. Rep. 188 363 (1990).

[2] J. Harris and B. Muller, Ann. Rev. Nucl. Part. Sci. 46 71 (1996).

[3] C.M.Ko and G.Q.Li , J. Phys. G: Nucl. Part. Phys. 22 (1673)
C.M.Ko, V.Koch and G.Q.Li, Ann. Rev. Nucl. Part. Sci. 47 509 (1997)

[4] Q. B. Pan and P. Danielewicz, Phys. Rev. Lett. 70, 2062 (1993).

[5] J. Zhang, S. Das Gupta and C. Gale, Phys. Rev. C 50, 1617 (1994).

[6] Ch.O.Bacri et al.,Int. Workshop on multiparticle correations and nuclear reactions, Nantea, France, p.338 (1994).

[7] J. Lukasik et al.,Phys. Rev C 55,1906 (1997).

[8] J. Aichelin, Phys. Reports 202, 233 (1991).

[9] L.G. Moretto, D.N.Delis and G.J. Wozniak,Phys.Rev.Lett.71,3935(1993).

[10] L. Phair et al., Phys. Rev Lett.75, 213 (1995); L.Phair et al.,Phys.Rev.Lett.**77**,822(1996)

[11] T.C.Sangter et al., Phys.Rev C 46, 1404(1992).

[12] D. R. Brown et al., Nucl. Phys. A 523, 386(1991).

[13] P. Roussel-Chomaz *et al*., Nucl. Phys. A 551, 508 (1993)

[14] K. Hagel *et al*., Phys. Rev. Lett. B 285, 10 (1992).

[15] J. P. Alard *et al*., Phys. Rev. Lett. 69, 889 (1992).

[16] G. Poggi *et al*., Nucl. Phys. A 586, 755(1995).

[17] M. Begemann-Blaich *et al*., Phys. Rev. C 48, 610 (1993).

[18] A. Schuttauf *et al*., Nucl. Phys A 607, 457 (1996).

[19] J.P.Hubble *et al*., Z. Phys A 340,263 (1991).

[20] A.S.Botvina *et al.*, Nucl. Phys. A 584, 737 (1995).

[21] C.A.Ogilvie *et al*., Phys. Rev. Lett. 67,1214(1991).

[22] J. Hubble *et al*., Phys. Rev. C 46, R1577 (1992).

[23] Ch. Hartnack, Ph.D Thesis, University of Frankfurt, Germany(1989).

[24] H.Stocker, L.P. Csernai, G.Buchwala, H.Kruse, R.Y. Cusson and W.Greiner, Phys. Rev.C25, 1873(1982).

[25] S.Hundan et.al, Phys. Rev. C71, 054604(2005).

[26] Yvez Schutz and Taps Collaboration, Nucl. Phys. A 599, 97(1996).

[27] J.Cleymans, H.Oeschler, K.Redlich, S.Wheaton, Phys. Lett. B 615,50(2005); T.Abbottetal, Phys. Rev. C 63, 064602(2001).

[28] M. Gazdzicki(NA Collaboration), J. Phys. G :Nucl. And Part. phys. 30,5701(2004) ; S.V. Afanasiev et al ;(NA 49 Collaboration), Phys. Rev. C666, 054902(2002).

[29] K.G.R.Doss, H.A. Gustafsson, H.Gutbrod, J.W. Harris, B.V. Jacak, K.H. Kampert, B.Kolb, A.M. Poskanzer, H.G. Ritter, H.R. Schimdt, L. Teitelbaum, M. Tincknell, S. Weiss, and H.Wieman, Phys. Rev. Lett 59,2720 (1987).

[30] W. Bauer, G.F. Bertsch, and H. Schulz, Phys. Rev, Lett. 69, 1888(1992).

[31] M. Begemann-Blaich *et al.,* Phys. Rev. C 48, 610(1993).

[32] D. Krofcheck, W. Bauer, G.M. Crawley, C. Djalali, S. Howden, A. Vander Molen, G.D. Westfall, R.S. Tickle, nad C. Gale, Phys. Rev. Lett. 63, 2028 (1989).

[33] R.W. Minich, S. Agrawal, A. Bujak, J. Chuang, A.S.Hirsch, N.T.Porile,B.C. Stringfelllow, and F.Turkot, Phys. Lett. B 118, 458(1982).

[34] H. Stocker and W. Greiner, Phys. Rep. 137,277(1986).

[35] K. T. R. Davies and S. E. Koonin, Ann. Of Phys. Rev C 23, 2042 (1981).

[36] A. K. Kerman and S. E. Koonin, Ann. Of Phys. 100, 332 (1976).

[37] E. Suraud, Ch. Gregoire and B. Tamain, Prog. Part. Nucl. Phys. 23, 357 (1989).

[38] A. R. Bodmer, C.N. Panos and A. D. Mackellar, Phys. Rev. C 22, 1025 (1980); L.Wilets, Y. Yariv and R. Chestnut, Nucl. Phys. A 301, 359 (1970).

[39] R. J. Lenk and V. R. Pandharipande, preprint University of Illinois; A. Vicentinni, G. Jacucci and V.R. Pandharipande, Phys. Rev. C 31, 1783 (1985).

[40] G. Peilert, A. Rosenhauer, J. Aichelen, H.Stocker and W. Geiner, Mod. Phys. Lett. A 3, 459 (1998).

[41] C.Hartnack, L.Zhuxia, L. Neise, G.peilert, A.Rosenhauer, H. Sorge, J. Aichelin, H. [44] Stocker and W. Greiner, Nucl. Phys. A 495, 303c (1989).

[42] E. Lehmann, R. K. Puri, A. Faessler, G. Batko and S.W. Huang, Phys. Rev. C 51, 2113(995).

[43] H. Feldmeier, Nucl. Phys. A 515, 147 (1990); J. Schnack, Ph. D. Thesis, GSI report, Darmstadt (1996); H. Feldmeir, K. Beller, Proc. I. Europ. Biennial Work-shop on Nucl. Phys., Megeve, France, World Scientific, S. 125 (1991); K. Beiler, Diplomarbeit, TH Darmstadt(1991).

[44] H. Feldmeir, J. Schnack, Proc. Int. Workshop on Dyn. Features of Nuclie, Spain (1993) World Scientific: H. Feldmeir, J.Schnack, Nucl. Phys. A 583, 347c (1995); H. Feldmeir, K. Bieler, J. Schnack, Nucl. Phys. A 586, 493 (1995).

[45] A. Bohnet, N. Ohtsuka, J. Aichelin, R. Linden and A. Faessler, Nucl. Phys. A 494, 349(1989).

[46] M. Trefz, A. Faessler and W. H. Dickhoff, Nucl. Phys. A 443, 499(1985).

[47] J. Cugnon and C. Hartnack and J. Aichelin, Phys. Rev. C 54(1993).

[48] A. Ono, H. Horiuchi, T. Maruyama and A. Ohnishi, Phys. Rev. Lett. 68, 2898 (1992); Prog. Theor. Phys. 87, 1185 (1992); Phys. Rev. C 47, 2652 (1993).

[49] A. Ono, H. Horiuchi, T. Maruyama, Phys. Rev. C 48, 2946 (1993); A. Ono, H.Horiuchi, Phys. Rev. C 51, 299 (1995); E. I. Tanaka, A. Ono, H. Horiuchi, T. Maruyama, A. Engel Phys. Rev. C 52, 316 (1995).

[50] J.P. Alard et al., Phys. Rev. Lett. 69, 889 (1992).

[51] M. Begemann-Blaich et al., Phys. Rev. C 48 ,610 (1993).

[52] C. A. Ogilvie et al., Phys. Rev. Lett. 67, 1214 (1991).

CHAPTER – 2

METHODOLOGY

2.1 Introduction

The study of intermediate energy heavy-ion collision needs correct treatment of the real and imaginary parts of nuclear interactions. The real part influences the trajectory of nucleons whereas the imaginary part deals with nucleon-nucleon collisions. In the following sections, we will discuss the Boltzmann-Uehling-Uhlenbeck (BUU) model, isospin Boltzmann-Uehling-Uhlenbeck (IBUU) model, the Quantum Molecular Dynamics (QMD) Model and the Isospin Quantum Molecular Dynamics (IQMD) Model.

2.2 Boltzmann – Uehling – Uhenbeck (BUU) Model

The BUU model[1,2,3] provides an equation for the phase space density $f(\vec{x}, \vec{p})$ of the nucleons, the constituents of the colliding nuclei. With the phase space density in hand, one can subsequently work out all the interesting observables that can later be compared to experimental data.

Let us consider first the (highly idealized) case where no collisions between the nucleons occur. Now, a basic theorem of (classical) statistical mechanics ("Liouville's Theorem") demands that $f(\vec{x}, \vec{p})$ has to be constant in time:

$$\frac{df}{dt} = \sum_{i=1}^{3}\left[\frac{\partial f}{\partial p_i}\frac{dp_i}{dt} + \frac{\partial f}{\partial q_i}\frac{dq_i}{dt}\right] + \frac{\partial f}{\partial t} = 0$$

Including the general Hamiltonian equations of classical mechanics (with a position and momentum dependent mean field potential $U(\vec{x},\vec{p})$), one obtains the Vlasov equation:

$$\left[\partial_t + \left(\nabla_{\vec{p}} U\right)\nabla_{\vec{x}} - \left(\nabla_{\vec{x}} U\right)\nabla_{\vec{p}}\right] f\left(\vec{x},\vec{p}\right) = 0$$

The Vlasov equation describes the time evolution of the phase space density in the presence of the mean field $U\left(\vec{x},\vec{p}\right)$. This mean field results from a self consistent treatment of the motion of the particles.

Thus, so far there are no collisions in the model. Besides, this treatment is completely classical. However, it is sometimes argued that quantum mechanical interactions alone are responsible for the generation of mean field potential $U\left(\vec{x},\vec{p}\right)$. The rest can be understood using classical physics.

Now it is clear that in a real heavy-ion reaction there are also collisions between the individual nucleons. Formally, the right hand side of the last equation does not vanish once collisions are taken into account. Considering only two-body collisions one gets the BUU equation:

$$\left[\partial_t + \left(\nabla_{\vec{p}} U\right)\nabla_{\vec{x}} - \left(\nabla_{\vec{x}} U\right)\nabla_{\vec{p}}\right] f\left(\vec{x},\vec{p}\right) =$$
$$\frac{4}{(2\pi)^3}\int d^3p_1 d^3p' d\Omega v \frac{d\sigma}{d\Omega}\delta\left(\vec{p}+\vec{p}_1-\vec{p}'-\vec{p}_1'\right)$$
$$\left[\begin{array}{l} f\left(\vec{x},\vec{p}'\right) f\left(\vec{x},\vec{p}_1'\right)\left(1-f\left(\vec{x},\vec{p}\right)\right)\left(1-f\left(\vec{x},\vec{p}_1\right)\right) \\ -\left(f\left(\vec{x},\vec{p}\right) f\left(\vec{x},\vec{p}_1\right)\left(1-f\left(\vec{x},\vec{p}'\right)\right)\left(1-f\left(\vec{x},\vec{p}_i'\right)\right)\right) \end{array}\right]$$

This equation governs the time evolution of the phase space density $f\left(\vec{x},\vec{p}\right)$ in the presence of the mean field potential $U\left(\vec{x},\vec{p}\right)$ and the two particle collisions. The term on the right hand side is the so called collision term. $\frac{d\sigma}{d\Omega}$ is the corresponding two-particle collision cross-section. The factors of the form $\left(1-f\left(\vec{x},\vec{p}\right)\right)$ in the collision term take the Pauli Principle into account, guaranteeing that no two particles occupy the same phase-space cell. This is in fact the only place where quantum mechanics explicitely enters the scene.

This equation is solved by test particle method. Here the phase space of each nucleon is represented by large number of pseudo-particles (called test particles). In its numerical implementation, the above equation reduces to a set of $6\times\left(A_T+A_P\right)\times\tilde{N}$ couple of first order differential equation in time. Here $\tilde{N}$ is the number of test particles per nucleon, A_T and A_P are the target and projectile mass number, respectively. The test particle method replaces the expectation value of single particle observable:

$$\langle O(t)\rangle = \int f(r,p,t)O(r,p)d^3rd^3p,$$

by a Monte Carlo integration

$$\langle O(t)\rangle = \frac{1}{n\left(A_T+A_p\right)}\sum_{i=1}^{n(A_T+A_P)}O\left(r_i(t),p_i(t)\right),$$

with r_i (t) and p_i (t) denote the points in phase space which are distributed according to f(r, p, t),

$$f(r,p,t)=\lim_{n\to\infty}\frac{1}{n\left(A_T+A_P\right)}\sum_{i=1}^{n(A_T+A_P)}\delta\left(r-r_i(t)\right)\delta\left(p-p_i(t)\right)$$

It is obvious that a large number of test particles will be needed to avoid the numerical noise. The test particles are treated as classical point particles. In recent calculations, one has also succeeded to use the Gaussian wave packet for test particles. These particles are then propagated under the classical Hamilton's equations of motion.

$$\dot{p}_i = -\frac{\delta\langle H\rangle}{\delta r_i},$$

$$\dot{r}_i = \frac{\dot{\delta}\langle H\rangle}{\delta p_i}$$

One should keep in mind that the forces acting on test particles are calculated from the entire distribution which includes the test particles of all events. In other words, the n parallel events are inter-connected and an event by event correlations cannot be analyzed within these models. In the limit $n \to \infty$, the distribution of these test particles represents a true one-body distribution function. Any one-body observable can be calculated by averaging the values weighted with the distribution function. In brief, the BUU model is able to explain the one body observables like collective flow, stopping and particle spectra, nicely. Due to lack of fluctuations and correlations, the N-body predictions are beyond the scope of this model.

2.3 Isospin - Boltzmann – Uehling – Uhenbeck (IBUU) Model

This is the Boltzmann-Uehling-Uhlenbeck (BUU) transport model which includes explicitly isospin degrees of freedom. The IBUU model treats protons and neutrons explicitly and includes an asymmetry term in the nuclear mean-field potential and a different scattering cross section for protons and neutrons. The model has been used recently to explain successfully several phenomena in heavy-ion collisions at intermediate energies which depend on the isospin of the reaction system [4]. Isospin – dependent BUU model solves the transport equation:

$$\partial_1 f_1 + \frac{\vec{p}}{E}\vec{\nabla}_r f_1 - \vec{\nabla}_r U \vec{\nabla}_p f_1 = \int \frac{d^3 p_1' d^3 p_2 d^3 p_2'}{(2\pi)^3} \sigma_{12} v_{12} (2\pi)^3 \delta^3\left(\vec{p}_1 + \vec{p}_2 - \vec{p}_1' - \vec{p}_2'\right) \times \left\{ f_1' f_2' (1 - f_1)(1 - f_2) - f_1 f_2 \left(1 - f_1'\right)\left(1 - f_2'\right) \right\}$$

The isospin dependence comes into the model through both the elementary nucleon-nucleon cross sections σ_{12} and the nuclear mean field *U*. Here we use the experimental nucleon-nucleon cross sections with explicit isospin dependence. The isospin resides in the fact that the cross section of neutron-proton collisions is about three times that of neutron-neutron or proton-proton collisions. We keep in mind, however, that in-medium cross sections and their isospin dependence might be strongly density dependent. The nuclear mean field *U* including the Coulomb and isospin symmetry terms is parametrized as :

$$U(\rho, \tau_z) = a\left(\frac{\rho}{\rho_0}\right) + b\left(\frac{\rho}{\rho_0}\right)^{\sigma} + (1 - \tau_z)V_C + C\frac{\rho_n - \rho_p}{\rho_0}\tau_z$$

In the above, ρ_0 is the normal nuclear matter density; ρ , ρ_n , and ρ_p are the nucleon, neutron, and proton densities, respectively; τ_Z equals 1 or -1 for neutrons or protons, respectively; and V_C is the Coulomb potential.

The IBUU and BUU models cannot describe phenomena such as cluster formation and multi-fragmentation produced in heavy ion collisions. But IBUU can describe the behaviour of collective flow such as collective rotation, and quantitatively and qualitatively explains the physical results.

2.4 Quantum Molecular Dynamics model (QMD):

In the quantum molecular dynamics (QMD) model [5-8], the nucleons are represented by Gaussian-shaped density distributions. They are initialized in a shape with a radius $R = 1.48\ A^{1/3}$, according to the liquid drop model. Each nucleon is supposed to occupy a volume, $\hbar^3$ so that the phase space is uniformly filled. The QMD model is an *n*-body

theory which simulates heavy ion reactions at intermediate energies on an event-by-event basis.

The total momentum in QMD is conserved because Hamiltoniun is well defined in the whole system. Apart from local Skyrme interaction V_{ij}^{loc} , a finite range Yukawa term V^{Yuk} and an effective Coulumb interaction V_{ij}^{Coul} are also included to account for various effects. The final potential reads as[9,10]:

$$V^{ij}=V_{ij}^{loc} + V_{ij}^{Coul} + V_{ij}^{Yuk} ,$$

The Yukawa term has been added to improve the surface properties of the interaction which are very important for multi-fragmentation. In nuclear matter where the density is constant , the interaction density coincides with the single particle density , and V_{loc} as well as V_{Yuk} is directly proportional to $(\frac{\rho}{\rho_0})$. The three-body part V_{loc}^{ij} of the interaction is proportional to $(\frac{\rho}{\rho_0})^2$.

In order to explain experimental results much better, the original version of the QMD model was improved to include isospin degrees of freedom explicitly and the isospin dependence as for Coulomb potential, symmetry potential, N–N cross sections and Pauli blocking which is known as the IQMD model.

In addition, initialization of projectile and target nuclei by using the nonlinear relativistic mean-field (RMF) theory, the neutrons and protons will be sampled in phase space separately because of the large difference between proton and neutron density distributions for nuclei far from the β stability line. The coordinates of the particle ground state and momentum distribution can be achieved by analysing the time evolution. Some isospin effects of heavy ion collisions at intermediate energies can be successfully explained with the IQMD model .

2.5 Isospin Quanmtum Molecular Dynamics Model (IQMD):

The IQMD model[11-13] can explicitly represent the many-body state of the system and contains correlation effects to all orders and all fluctuations. It has basically two advantages:

(1) many-body process, in particular, the formation of complex fragments is treated and

(2) the model allows for an event-by-event analysis of heavy ion reactions .

In order to describe the isospin effects of the dynamical process of HIC, quantum molecular dynamics (QMD) should be modified properly:

(1) the density dependent mean field should contain the correct isospin-dependent terms including symmetry potential and Coulomb potential,

(2) the in-medium N-N cross section should be different for neutron-neutron (proton-proton) and neutron-proton collisions, and finally,

(3) Pauli blocking should be counted by distinguishing neutron and proton.

Initialisation:

In IQMD model, centroid of each Gaussian (in a nucleus) is randomly distributed in a phase space sphere ($r \leq R$ and $\rho \leq \rho_f$) with R = 1.48 $A^{1/3}$ Fermi corresponding to ground state density ρ_0 = 0.17fm^{-3} . The fermi momentum ρ_F depends on the ground state density. For ρ_0=0.17 fm^{-3} , the value of ρ_F is $\approx$ 268 MeV/c. Due to this collision , nucleons close to surface (where the local potential energy is low) are unbounded initially.

As a result, binding energy per nucleon is low as compared to Weizsacker mass formula. Therefore, the initialised nuclei are less stable against suporius particle evaporation compared to oriented QMD model.

Potentials used in IQMD:

The IQMD-model offers rather stable density distributions and good energy conservation, however for the price of nucleon evaporation and improper binding energies (E_{bind} = 4-5MeV/nucleon for heavy nuclei instead of 8 MeV/nucleon).

In IQMD model, each nucleon is represented by a Gaussian wave packet of the form:

$$f_i(\vec{r},\vec{p},t) = \frac{1}{\pi^3\hbar^3} \times e^{[-(\vec{r}-\vec{r_i}(t))^2 \frac{2}{L}]} \times e^{[-(\vec{p}-p(t))^2 \frac{L}{2\hbar^2}]}$$

The total one nucleon Weigner density is, therefore, the sum of all nucleons. The expectation value of Hamiltonian is :

$$\langle H \rangle = \langle T \rangle + \langle V \rangle$$

$$= \sum_i \frac{p_i^2}{2m_i} + \sum_i \sum_{j>i} \int f_i(\vec{r},\vec{p},t) V^{ij}(\vec{r}',\vec{r}) \times f_j(\vec{r}',\vec{p}',t) d\vec{r}\, d\vec{r}'\, d\vec{p}\, d\vec{p}'$$

The baryon-baryon potential V^{ij} consists of real part of Bruckner G-matrix which is supplemented by an effective Coulumb interaction acting between the charged particles. The former part can be parameterised in term of Skyrme type interaction to finite range Yukawa potential as well as momentum dependent contribution. In addition, a symmetry potential between protons and neutrons corresponding to the Bethe-Weizsacker formula has been included. Therefore, V^{ij} consists of:

$$V^{ij} = G^{ij} + V^{ij}_{Coul}$$

$$= V^{ij}_{Skyrme} + V^{ij}_{Yukawa} + V^{ij}_{Coul} + V^{ij}_{mdi} + V^{ij}_{sym}$$

$$= t_1\delta(\vec{x}_i - \vec{x}_j) + t_2\delta(\vec{x}_i - \vec{x}_j)\rho^{\gamma-1}(\vec{x}_i) + t_3 \frac{\exp\left(\frac{-|\vec{x}_i - \vec{x}_j|}{\mu}\right)}{\frac{|\vec{x}_i - \vec{x}_j|}{\mu}} +$$

$$t_4 \ln^2(1 + t_5(\vec{\rho}_i - \vec{\rho}_j)^2)\delta(\vec{x}_i - \vec{x}_j) + \frac{Z_i Z_j e^2}{|\vec{x}_i - \vec{x}_j|} +$$

$$t_6 \frac{1}{\rho_0} T_3^i T_3^j (\vec{r}_i - \vec{r}_j)$$

In the description of the Coulomb interaction V^{ij}_{Coul}, Z_i, Z_j are the charges of the baryons i and j.

The momentum dependent V^{ij}_{mdi} of the NN interaction, which may optionally be used in the model, is obtained from a fit to the experimental data [14,15] on the real part of the nucleon optical potential which yields .

$$U_{mdi} = \delta.\ln^2(\varepsilon.(\Delta\vec{p})^2 + 1).(\frac{\rho_{\text{int}}}{\rho_0})$$

The asymmetry energy is taken into account by the term

$$V^{ij}_{sym} = t_6 \frac{1}{\rho_0} T_3^i T_3^j \delta(\vec{r}_i, \vec{r}_j),$$

where T_3^i and T_3^j denote the isospin T_3 of particles i and j, i.e. 1/2 for protons and -1/2 for neutrons. The constant t_6 = 100 MeV.

2.6 Cluster Analysis:

The minimum spanning tree method (MST) [16-20] is used in cluster analysis and track finding, if we consider tracks to be clusters of points. In MST, two nucleons share the same fragment if their centroids are closer than a distance d_{min},

$$| r_i - r_j | \leq d_{\min},$$

where r_i and r_j are the spatial positions of both nucleons. The minimum distance d_{min} has been used as a free – parameter which varies between 2-4 fm. Its influence on multifragmentation (at 200 – 300 fm/c) is reported to be small. This approach (being a spacial approach cannot detect different fragments which are (almost) overlapping and therefore, will give a single big fragment during early stage of the reaction where density is quite high and the interactions among nucleons are still active. One simulates the reaction using IQMD. Then special distance of all nucleons is checked. A nucleon is part of a fragment if there is another one within a distance of r_{min} = 4 fm.

2.7 Objective of the work:

Ever since the first observation of collective flow at the Bevalac by the Plastic Ball Collaboration [21], a systematic investigation of collective phenomenon in heavy-ion reactions has been pursued at many accelerators. The different bombarding energies at the various accelerators create different demands on the experimental setup because of the widely varying multiplicities and the momenta of the outgoing reaction products. Furthermore, the different types of flow under study have different implications for phase space coverage. On the other hand, for longitudinal and radial transverse flow, large acceptance in momentum p_t and rapidity y for different particles is important. The sideflow and elliptic flow, on the other hand, require a uniform coverage of the azimuthal angle for correct reconstruction of the reaction plane. In order to investigate the flow behaviour of specific particles, limited additional coverage in transverse momentum and rapidity is

sufficient. Indeed, the general trend in these experiments is to cover the full phase space as completely as possible. Most of the systematics on flow is derived from the study of symmetric collisions. Here, by symmetry arguments, it is sufficient to measure either at forward or backward rapidity with respect to midrapidity.

In the regime below 100 A MeV, the angular momentum transferred by the projectile enhances the emission of particles in the reaction plane. They are emitted from the fast-spinning compound nucleus formed in a deep inelastic collision. The azimuthal distribution of those particles can therefore be characterized by a positive elliptic flow. In collision of larger systems, such as Xe + Au at 50 A MeV, pronounced signals of this flow component has been measured via two-particle angular correlation functions. The elliptic flow component increases monotonically as collision become more peripheral, and vanishes for the most central collisions. The monotonic centrality dependence favours the interpretation that the angular momentum is the major cause of the elliptic flow, since the pressure is expected to play a minor role in this energy regime. However, at beam energies below 50 AMeV, the elliptic flow is still gets stronger, indicating that the attractive nuclear potential is enhancing the rotation. The measurement of the two-particle angular correlation functions for various particles exhibits a monotonic increase of the elliptic flow signal with the mass of the particle, as is observed for the transverse flow component.

There are several detectors used to study collective flow phenomenon. FOPI at the SIS (GSI) is a typical detector with nearly 4π coverage and full azimuthal symmetry using a solenoidal magnetic field for tracking. The experiment E877 at the AGS (Brookhaven National Laboratory), is a typical setup with spectrometer and good centrality measurement like KaoS [22], E802 [23], and NA44 [24]. The experiment NA49 at the SPS (CERN), is a representative of 4π tracking devices in large dipole magnets similar to EOS, E895 [25], and E810 [26].

The study of collective transverse flow in nucleus-nucleus collisions can provide information about the nuclear equation of state (EOS). Using QMD model, collective

transverse flow has been described in terms of nucleon-nucleon scattering in a nuclear mean field. It was predicted that collective transverse flow in the reaction plane disappears at an incident energy, termed as the balance energy, where the attractive scattering (dominant at energies around 10MeV/nucleon) balances the repulsive interactions (dominant at energies around 400 MeV/nucleon). The measurement of impact parameter dependence of the balance energy with predictions from QMD was studied in [27]. Balance energy was measured for ${}^{40}_{18}Ar+{}^{45}_{21}Sc$ and ${}^{58}_{26}Fe+{}^{58}_{26}Fe$ for six reduced parameter bins. Also the experimental values of balance energy plotted against impact parameter were given. The values of balance energy and impact parameter were used in our calculations using IQMD. In this thesis our aim is to pin down the effect of isospin component on the elliptical flow. Here ${}^{40}_{18}Ar+{}^{45}_{21}Sc$ system is studied using energies 85, 95, 105, 110, 115, 130 MeV/nucleon at $\hat{b}$ = 0.28, 0.39, 0.48, 0.56, 0.62, 0.76. Also ${}^{58}_{26}Fe+{}^{58}_{26}Fe$ system is studied using energies 73, 75, 84, 90 MeV/nucleon and at $\hat{b}$ = 0.28, 0.39, 0.48, 0.56.

2.8 References:

[1] G.F. Bertsch, W. Cassing and U. Mosel, Phys. Rev. C 29, 673(1984).

[2] J. Aichlen, C. Hartnack, A. Bohnet, L.Zhuxia, G. Peilert, H. Stocker and W. Greiner, Phys. Lett. B 224, 34(1989).

[3] W. Bauer, G.F. Bertsch, W. Cassing and U. Mosel, Phys. Rev. C 34, 2127 (1986).

[4] B. A. Li and S. J. Yennello, Phys. Rev. C 52, R1746 (1995).

[5] J. Aichelin, A. Rosenhauer, G. Peilert, H. StÄocker, and W.Greiner. Phys. Rev. Lett. 58, 1926 (1987).

[6] J. Aichelin and H. StÄocker. Phys. Lett. B176, 14 (1986).

[7] G. Peilert, H. StÄocker, A. Rosenhauer, A. Bohnet, J. Aichelin and W. Greiner. Phys. Rev. C39, 1402 (1989).

[8] J. Aichelin. Phys. Reports 202, 233 (1991).

[9] H. Feldmeier. Nucl. Phys. A515, 147 (1990).

[10] A. Ono, H. Horiuchi, T. Maruyama and A. Ohnishi. Phys. Rev. Lett.

68, 2898 (1992).

[11] C. Hartnack, L. Zhuxia, L. Neise, G. Peilert, A. Rosenhauer, H. Sorge, J. Aichelin, H. StÄocker, and W. Greiner. Nucl. Phys. A495, 303 (1989).

[12] Ch. Hartnack, J. Aichelin, H. StÄocker and W. Greiner. Mod. Phys. Lett. A9, 1151 (1994).

[13] S. So et al. Phys. Rev. C 51, 3320 (1995).

[14] L. G. Arnold et al. Phys. Rev. C25, 936 (1982).

[15] G. Passatore. Nucl. Phys. A95, 694 (1967).

[16] J. Aichelin, Phys. Reports 202, 233 (1991).

[17] A. Bohnet, N. Ohtsuka, J. Aichlen, R. Linden and A. Faessler, Nucl. Phys. A 494, 349 (1989).

[18] D. T. Khoa, N. Ohtsuka, A. Faessler, M. A. Matin, S. W. Huang, E. Lehmann and Y. Lofty, Nucl. Phys. A 542, 671 (1992).

[19] P. B. Gossiaux and J. Aichelin, Phys. Rev. C 56, 2109.

[20] S. Kumar and R. K. Puri, Phys. Rev. C 58, 320 (1998).

[21] A. Baden, et al. Nucl. Instrum. Methods A 203 : 189 (1982).

[22] P. Senger, et al. Nucl. Instrum. Methods A 327 :393 (1993).

[23] T. Abbott, et al Nucl. Instrum. Methods A 290 :41 (1990).

[24] H.Boggild, et al. Phys. Lettt. B302 :510 (1993).

[25] G. Rai, et al IEEE Trans. Nucl. Sci. 37 :56 (1990).

[26] A Etkin, et al. IEEE Trans.Nucl.Sci. 36 :58 (19991).

[27] Nuclear Physics A681,343c-350c (2001).

CHAPTER – 3

PHASE SPACE ANALYSIS

3.1 Introduction

In the preceding chapters, we studied the detail of heavy ion reactions. At low incident energies, fusion is more probable where as at intermediate energies multifragmentation dominates. At high incident energies, a clear evaporation is seen. In the following sections, we will present phase space simulations of heavy ion collisions and the relation of nuclear matter density at the time of collision and the rate of nucleon-nucleon collisions as a function of time. In this chapter, the variation of phase space with time has been studied.

3.2 Snap – shots of the phase space

Here we will survey the evolution of heavy ion reaction. One way to look at phase space is to study the phase – space in X–Y and X–Z planes In figure 3.1. and 3.2, we display the time evolution of ${}^{58}_{26}Fe+{}^{58}_{26}Fe$ collisions at E = 20 MeV/nucleon and $\hat{b} = 0.3$ in coordinate and momentum space respectively. Here both front and side views are displayed. The front and side views are quite different pictures for a non-central collision. Two nuclei are far apart in X–Z plane, whereas they are overlapping in X–Y plane.

During the initial stages of the reaction, projectile and target are well separated both in coordinate and momentum space and as a result, whole of the matter is in the form of spectator matter only. This is called the initial phase. As the nuclei overlap, the density increases, that leads to more and more collisions that changes the interacting matter from spectator to participant one. Because of the impact parameter ($\hat{b} = 0.3$), some of the nucleons (spectators) never undergo a collision with nucleons of the collision partner because of the

geometry of the collision. These nucleons experience only the (distorted) mean field of their parent nuclei and propagate with little deflection. If we increase the impact parameter, we will notice a reduced intensity of participant matter.

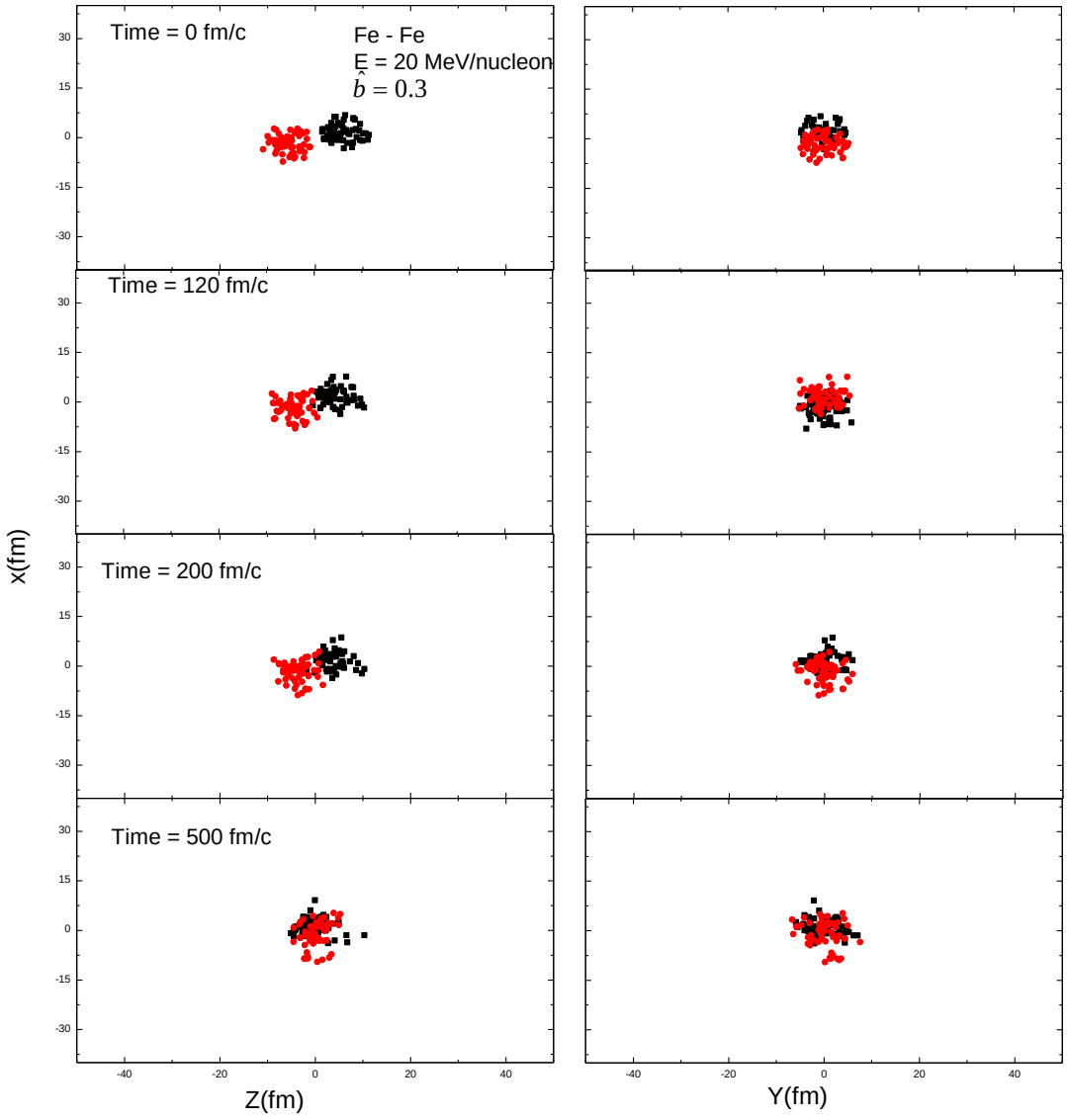

Figure 3.1 : The evolution of the ${}^{58}_{26}Fe+{}^{58}_{26}Fe$ reaction at $\hat{b} = 0.3$ and incident energy of 20 MeV/nucleon. This plot is a projection of spacial space into (X–Z) & (X–Y) planes.

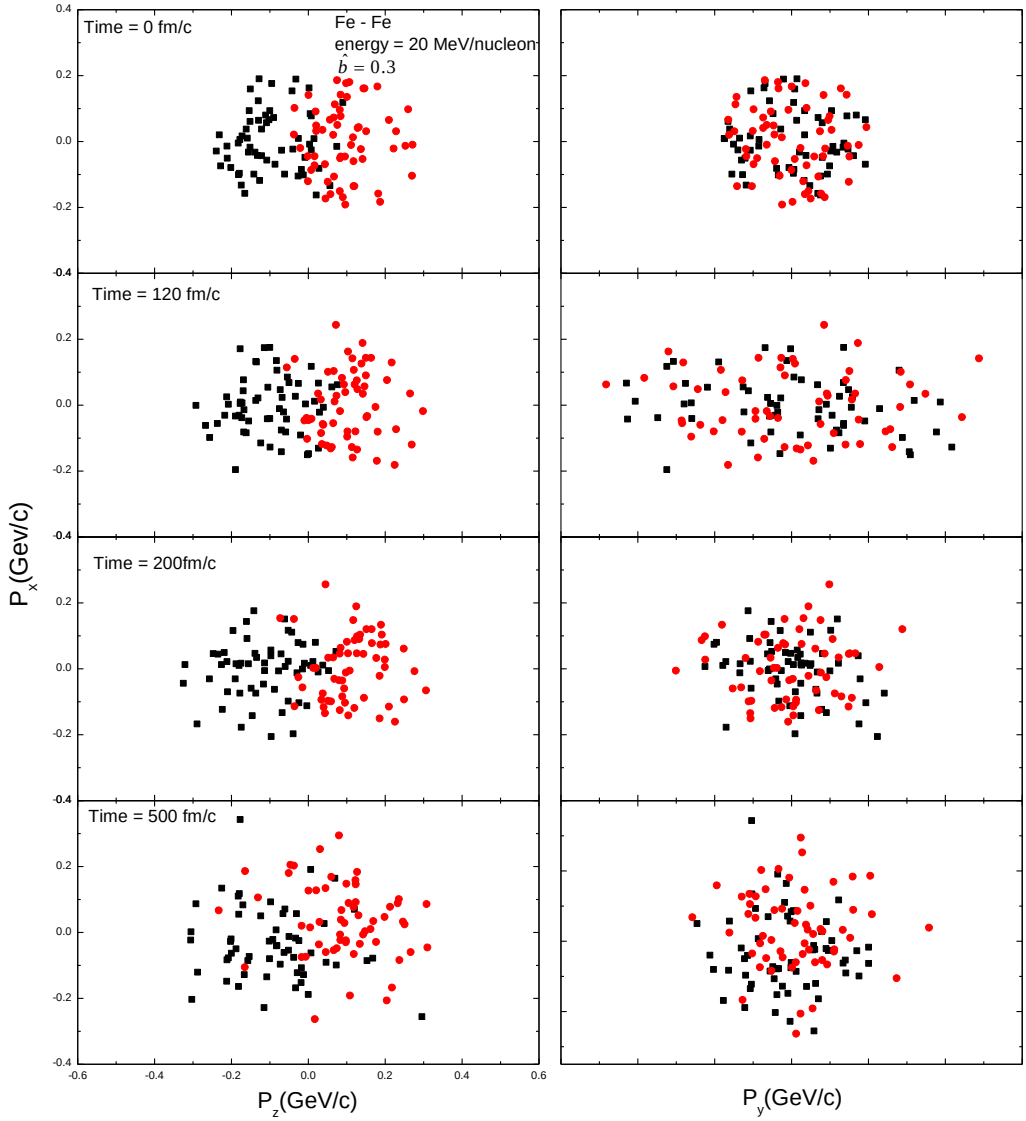

Figure 3.2 : Same as fig. 3.1 but in momentum space.

After the collision, the formation of light particles and heavy fragments can be seen. In contrast, the momentum space is less affected. The beam energy is too small to allow

nucleon-nucleon collision to take place and hence no substantial change in momentum space occurs.

The next stage in the reaction scenario is the relaxation of the energy density. The central system is undergoing expansion, thereby reducing its temperature and density. Due to frequent nucleon-nucleon collisions, nucleons scatter in the transverse direction. With the evolution of the reaction, participant matter increases, leading to more nucleons scattering in the transverse direction. Therefore, after the collision, the formation of light particles and heavy fragments can be seen [1-3]. At the end of the reaction, we see only a few spectator nucleons. Looking at the momentum space (Fig. 3.2), we see that the spectator nucleons have very little change in their initial velocity profile over the period of reaction.

On the other hand, participant matter push the matter into midrapidity region, therefore, driving the system into global equilibrium. Naturally, more the initial correlations are destroyed, more is the system close to global equilibrium. Since, these figures are the snapshots of a single event, the picture could be slightly different for different events. In the final state, matter is cold and fragmented, therefore, this may lead to the expansion of compressed matter which breaks into pieces due to Coulomb instabilities. The system always expands into the direction of the largest gradients in density and temperature

The reaction stops at a point commonly referred to as freeze-out. At this point the densities are small enough that during a typical path length no further interaction will occur. Our phase space is similar to phase space shown in ref. [4, 5, 6].

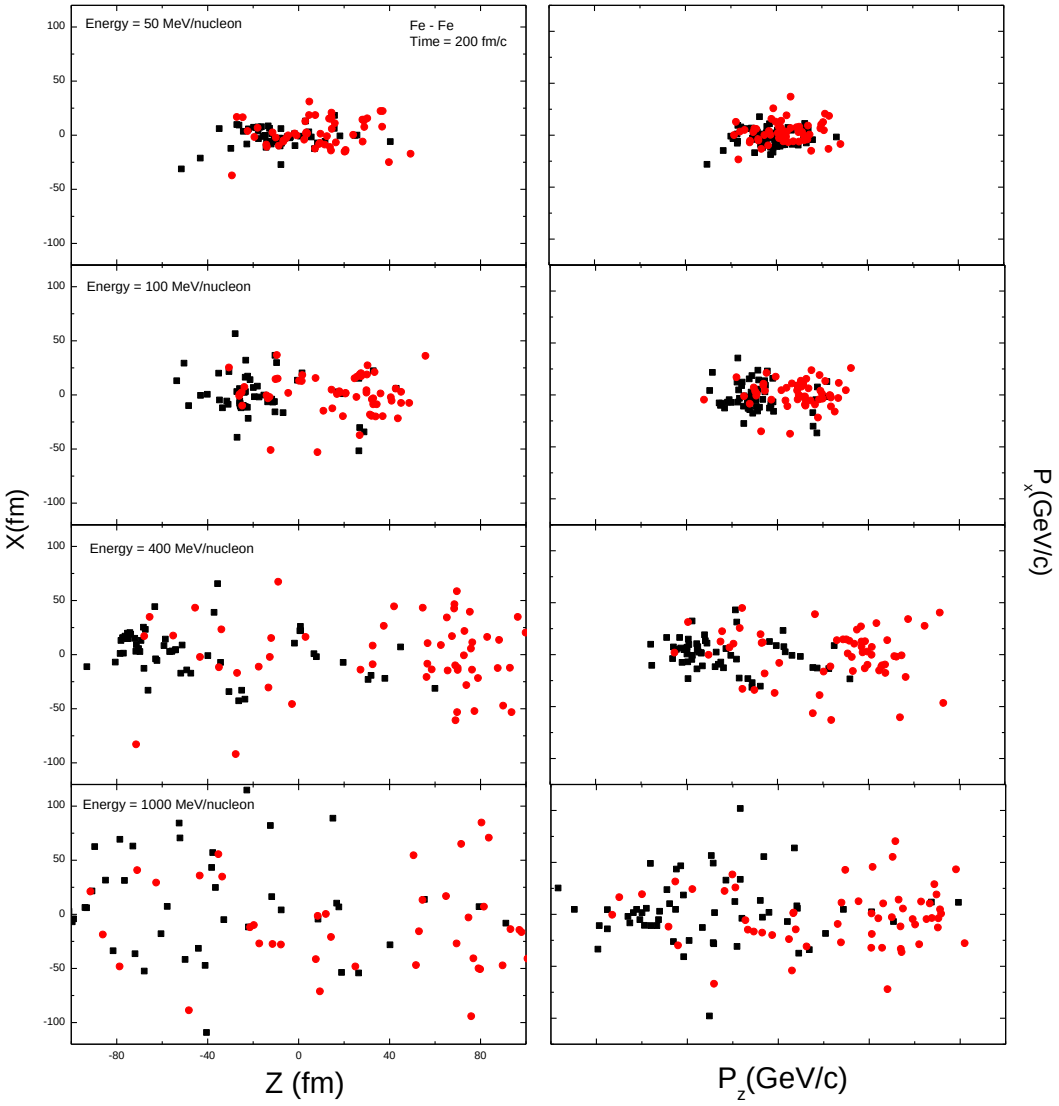

Figure 3.3 : The evolution of the phase-space in Fe-Fe collisions at incident energies E = 50 MeV/nucleon, 100 MeV/nucleon, 400MeV/nucleon and 1000MeV/nucleon, respectively at impact parameter $\hat{b} = 0.52$ fm. This plot is a projection of spacial and momentum space into (X-Z) and (P_x–P_z) planes.

The role of different incident energies is displayed in figure 3.3 where the X-Z & P_x - P_z coordinates of all nucleons are plotted at 200 fm/c. A very heavy fragment can be seen at 50 MeV which disappears at higher incident energies. At 1 GeV/nucleon, nearly no fragment survives. The P-space at 50 MeV is quite compact whereas two different momentum – spaces can be seen at 1 GeV/nucleon. In other words, the present figure depicts that at low incident energies, a partial fusion can occur whereas at higher energies either emission of the light fragments or free nucleons will dominate the reaction. Such change in fragment sizes also occur with change in incident energes of projectile [7].

3.3 The Time evolution

A heavy ion collision can be thought as exploring a path in phase diagram depending on incident energy and colliding nuclei. It proceeds from initial normal nuclei at saturation density at more or less asymmetry, to high density and heated nuclear matter at maximum compression to dilute nuclear matter in the expansion stage. Flow and particle production are best suited for high density phases.

The final form of the nuclear matter is closely related to the density of collision. Matter density is calculated by [8].

$$\langle \rho(r) \rangle = \left\langle \sum_j \frac{1}{(2\pi L)^{3/2}} e^{-(\vec{r}_i - \vec{r}_j)^2 / 2L} \right\rangle$$

The above density definition shows the number of nucleons in the vicinity of each nucleon. In actual calculations, we take a sphere of 2 fm radius around the centre of mass and compute the density at each step during the reaction using the above equation.

Fig. 3.4 shows the evolution of density as a function of time. We also display the rate of collisions at different bombarding energies. We notice that the density is closely related to the violence of collisions. The final stage density is quite different at different incident energies. It is highest at 20 MeV/nucleon and is least at 1000 MeV/nucleon. There is

a gradual decrease in the density with increase in the bombarding energy. At high energy, the collision among the nucleons are violent, so low density is reached and number of collisions are very high as compared to low energy collisions.

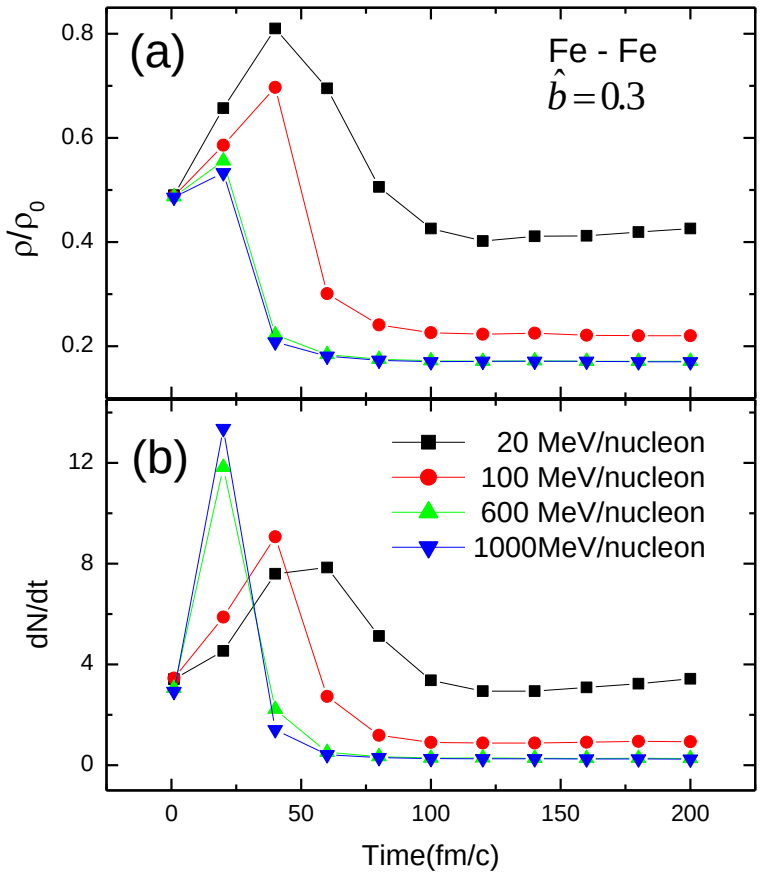

Fig 3.4: (a) The evolution of mean density as a function of time. (b) The evolution of the rate of nucleon – nucleon collisions as a function of time. Here different lines shows the same results, but at different bombarding energies.

When the incident energy is higher, the reaction finishes much earlier compared to the reaction simulated at relatively lower energies.

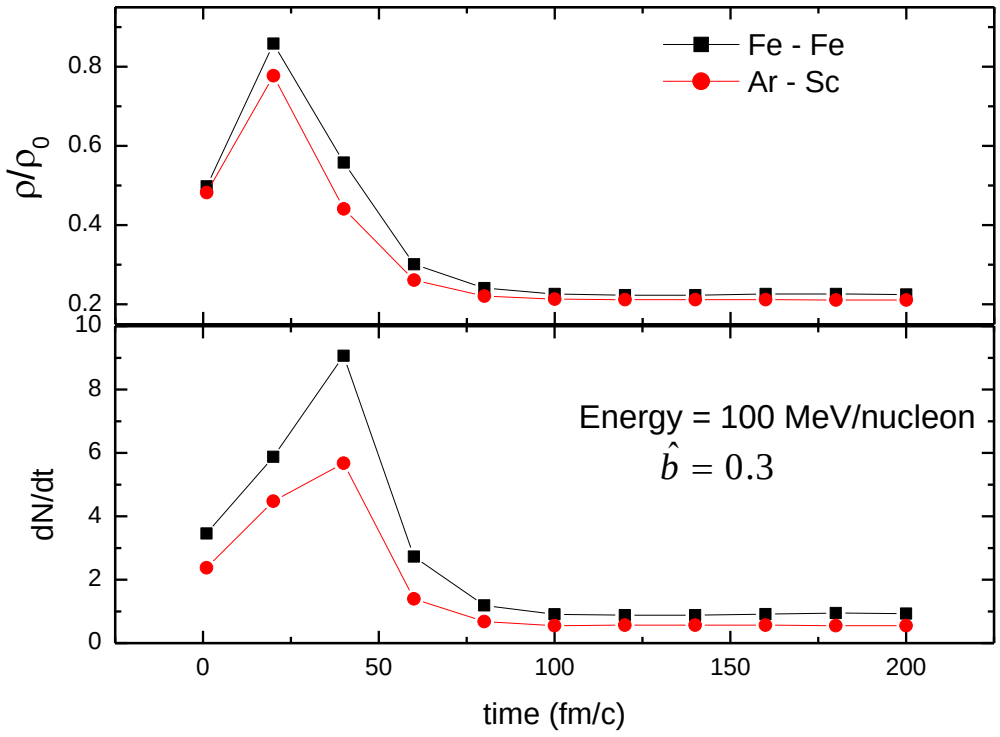

Fig 3.5: The evolution of the mean density and rate of nucleon-nucleon collisions as a function of time for ${}^{40}_{18}Ar+{}^{45}_{21}Sc$ and ${}^{58}_{26}Fe+{}^{58}_{26}Fe$.

The saturation time of the density depends strongly on the masses of colliding nuclei. For heavy masses it will take far more time before the density saturates. Thus the reaction saturation time is smaller for the lighter nuclei compared to the heavier ones. Fig 3.5 shows the relationship of density and rate of collisions of systems of different masses. The wider density zone in heavier colliding nuclei (${}^{58}_{26}Fe+{}^{58}_{26}Fe$) over a long time span indicates the ongoing interactions among the nucleons which is in agreement with [9]. Also due to larger interaction volume in heavy nuclei, the interactions among nucleons continue for a longer time which is also evident from the density profile. Further, a finite extended density zone in heavier nuclei leads to more nucleon – nucleon collisions. Maximal size varies linearly with increase in size of interacting nuclei [10,11].

3.4 References

[1] S.Kumar & R.K. Puri, Physical Review C, Volume 60, 054607 (1999).

[2] J.Singh, S. Kumar & R.K. Puri, Phys. Rev. C. Volume 63, 054603 (2001)

[3] S. Kumar & R.K. Puri, Phys. Rev. C 58, 320 (1998).

[4] R. K. Puri & J. K. Dhawan, Eur. Phys. J. A. 33, 57-64 (2007).

[5] R. K. Puri & J. K. Dhawan, Physical Review 74, 054610 (2006).

[6] R. K. Puri & J. K. Dhawan, Physical Review 75, 057601 (2007)

[7] P.B. Gossia, R.K. Puri, C.Hartnak & J. Aichelin, Nucl. Phys. A 619, 379 (1997).

[8] D.T. Khoa et al., Nucl. Phys. A 548, 102 (1992); R.K. Puri et al., Nucl. Phys. A 575, 733 (1994).

[9] Aichelin, Phys, Rep. 202, 233 (1991).

[10] A.D. Sood and R.K. Puri, Phys. Rev. C 70, 034611 (2004).

[11] B. Blattel et. Al. Phys. Rev. C 43, 2728 (1991).

CHAPTER – 4

ELLIPTIC FLOW

4.1 Definition of Collective Motion

In order to establish and describe the quasimacroscopic properties of nuclear matter, it is necessary to investigate collective observables. Collectivity in this context means that a number of ejectiles exhibit a common property (e.g. the emission of many particles of the same kind or the emission of many ejectiles with a common velocity field or into a common direction). Restricting this very general definition of collective behavior to kinematics observables leads to the definition of collective flow: Any common feature of all ejectiles emitted in a heavy-ion collision can be taken as an indicator for the underlying nuclear-matter phase distribution. There are several collective phenomenon which are defined below:

1. "Longitudinal flow" describes the collective motion of the particles in their original direction defined by the beam.
2. "Radial flow" characterizes particles that are emitted from a source with a common velocity field independent of the direction, i.e. for a velocity field with spherical symmetry.
3. "Transverse flow" is the term used whenever the velocity field is found to be independent of the azimuthal angle.
4. The orientation of the impact parameter vector in the nucleus-nucleus collisions defines one specific azimuthal direction. An enhanced emission into this direction is experimentally observed. This most prominent directed flow phenomenon is called "sideflow".

5. “Elliptic flow” describes an emission pattern in which particles are found to be preferentially emitted with respect to a certain azimuthal angle and with back-to-back symmetry.

4.2 Time Evolution

In order to define more clearly the most relevant quantities for collective motion in heavy-ion collisions, figure 4.1 sketches schematically a typical heavy-ion reaction. When two nuclei approach each other, their orientation in space and the initial beam direction define the reaction plane. The impact parameter vector beam is located in the reaction plane.

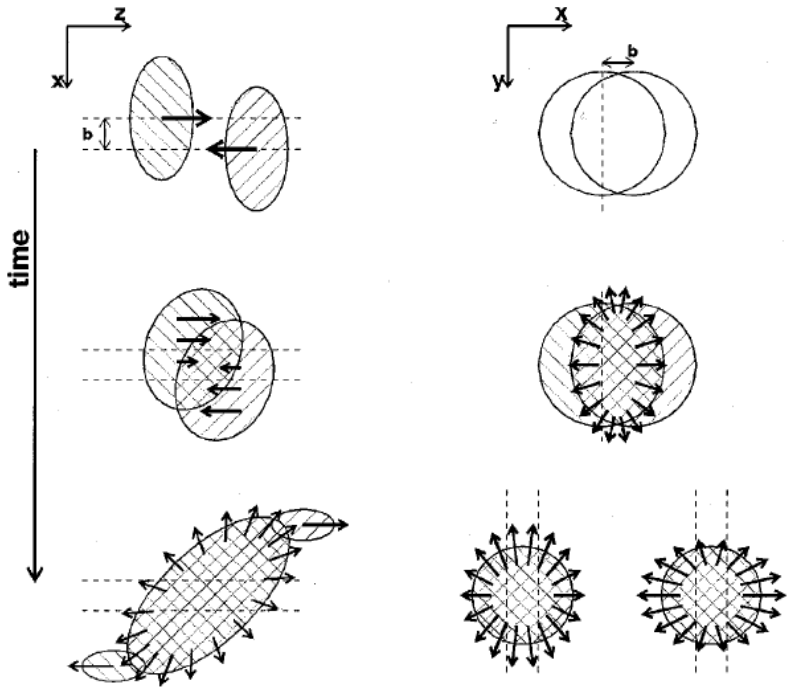

Figure 4.1: Schematic view of the time evolution in a heavy-ion collision and the development of collective velocity fields. *Left*, the time evolution of the reaction in the reaction plane. *Right*, a sketch of the transverse plane at midrapidity. Several phases of a typical heavy-ion reaction can be defined.

1. **Initial Phase** : When the two matter distributions approach each other and start to overlap, the properties of the NN interaction in free space will be visible in the scattering process. Nucleons at the surfaces will reflect the Lorentz-force-like behavior of the NN interaction most directly. They will be deflected outward and, because of symmetry for finite impact parameter, will show an enhancement in the reaction plane.

2. **High Density Phase**: Once the matter distributions of the projectile and target overlap (Figure 4.1, *central row*), the properties of the NN interaction are not well known. A zone of high density is formed. Many-body effects that are present even at normal nuclear-matter densities can occur, as well as modifications of the properties of the constituents. For large systems and large enough cross sections, the overlap zone developed into a system characterized by an initial baryon number and energy density. Depending on its EOS, which relates the pressure to density and temperature, the overlap zone may reach conditions that are described by an average density and temperature. This process of heating and compressing is intimately connected to the question of stopping, namely how much energy of the original longitudinal motion is transferred into internal degrees of freedom in the course of the reaction. Having stored part of the available energy in compression and thermal excitation, heavy-ion collisions produce unique conditions of nuclear matter that are not accessible otherwise. It should be noted that, for a finite impact parameters, some of the nucleons (spectators) never undergo a collision with nucleons of the collision partner because of the geometry of the collision. Those nucleons experience only the (distorted) mean field of their parent nuclei and propagate with little deflection. They do, however, play a crucial role in diagnosing the properties of central collision zone.

3. **Expansion**: The next stage in the reaction scenario is the relaxation of the energy density. The central system is undergoing expansion, thereby reducing its temperature and density. For symmetric reasons, the expansion is azimuthally symmetric for central collisions.

For reactions with finite impact parameter, where an oriented velocity might have survived the compression phase, the situation is much more complicated. The expansion now has a directed velocity field superimposed (Figure 4.1, *lower left*). The system always expands into the direction of the largest gradients in density and temperature. Inspection of the geometry depicted in Figure 4.1 reveals that, in transverse direction, the initial expansion is largest in the direction of reaction plane. In longitudinal direction, the expansion scenario depends on the degree of stopping.

4. **Freeze-Out** : The reaction stops at a point commonly referred to as freeze-out. At this point the densities are small enough that during a typical path length no further interaction will occur.

4.3 Elliptic flow

Elliptic flow [1-4] develops because of almond shape of the overlapping region in a heavy ion collision. The schematic diagram of elliptic flow is shown in figure 4.2. Elliptical or higher order azimuthal shapes can provide help (a) when the phase space coverage is limited to a narrow region around midrapidity, and (b) at beam energies close to the balance energy, where no net deflection of nucleons is observed. The elliptic flow is expected to be larger in peripheral collisions because of the anisotropy in coordinate space which is the source of this flow.

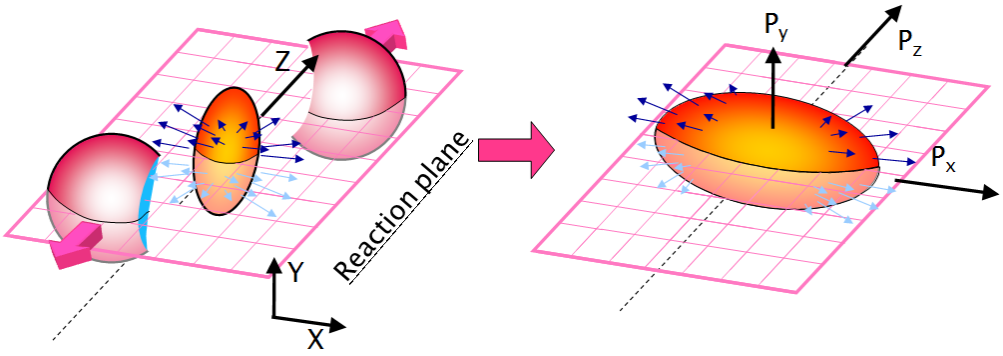

Figure 4.2 : Pictorial representation of elliptic flow

The study of elliptic flow provides valuable data on the nuclear equation of state and isospin dependent N-N cross section. Study of dependence of elliptic flow and different fragment flows on beam energies, mass number, isospin and impact parameter have revealed quite interesting physics about the properties and origin of collective flow.

The anisotropic flow [5-9] is defined as the different n^{th} harmonic coefficient v_n of an azimuthal Fourier expansion of the particle invariant distribution.

$$\frac{dN}{d\phi} \propto 1 + 2\sum_{n=1}^{\infty} v_n \cos(n\phi)$$

where ϕ is the azimuthal angle between the transfer momentum of the particle and the reaction plane. In the coordinate system the z axis is along the beam axis and the impact parameter axis is labelled as x-axis.

The first harmonic coefficient v_1 represents the directed flow.

$$v_1 = <\cos\phi> = \frac{p_x}{(p_x^2 + p_y^2)^{1/2}}$$

The parameter of elliptic flow is quantified by the second order Fourier coefficient:

$$v_2 = \langle \cos(2\phi) \rangle = \frac{p_x^2 - p_y^2}{p_x^2 + p_y^2}$$

The azimuthal distribution with respect to the reaction plane were fitted using a truncated Fourier expansion:

$$\frac{dN}{d\phi} \approx [1 + 2v_1 \cos(\phi) + 2v_2 \cos(2\phi)]$$

where ϕ is the azimuthal angle of the emitted particle momentum relative to the x axis.

Positive values for <cos 2ϕ> reflect a preferential in-plane emission, and negative values for <cos 2ϕ> reflect a preferential out-of-plane emission.

The elliptical flow parameters are determined by the complex interplay among expansion, rotation and the shadowing of spectators. Both the mean field and two-body collision parts play important role at this energy region. The mean field plays dominant role at low energies and then gradually the two body collision part becomes dominant with increasing energy.

The transition energy of elliptic flow at intermediate energies may be particularly useful in extracting the information on the nuclear effective interaction. While the elliptic flow at the energies higher than the transition energy will be useful to extract the medium correction of nucleon-nucleon cross sections because two-body collisions play more important role on collective flow at these energies.

The elliptic flow results from a competition between the early squeeze-out when the compressed matter tries to move out in the direction perpendicular to the reaction plane and the late-stage in-plane emission associated with the shape of the participant zone. The

squeeze-out contribution to the elliptic flow depends on the pressure built up early on, compared to the energy density.

Thus, a detailed study on the excitation function of elliptical flow can provide more useful information on the nucleon-nucleon interaction related to the equation of state of nuclear matter and the medium correction of nucleon-nucleon cross sections.

4.4 Results and Discussion

Here simulation of the reactions of ${}^{40}_{18}Ar+{}^{45}_{21}Sc$, ${}^{58}_{26}Fe+{}^{58}_{26}Fe$ is done at incident energies between 85 and 130 MeV/nucleon. As noted in ref. [10], relativistic effects donot play role at these incident energies and the intensity of sub-threshhold particle production is very small. The phase space generated by the IQMD has been analysed using minimum spanning tree (MST) [11] method. The MST method binds two nucleons in a fragment if their distance is less than 4 fm. In recent years, several improvements have also been suggested[12].

If $v_2 > 0$, it describes the eccentricity of an ellipse like distribution and indicates in-plane enhancement of the particle emission, a rotational behavior. On the other hand, a negative value of v_2 shows the property of squeeze out effect perpendicular to the reaction plane. Obviously, zero value of v_2 corresponds to an isotropic distribution in the transverse plane. The v_2 is generally extracted from the midrapidity region. The particles corresponding to $Y_{c.m.} \geq 0$ has been defined as projectile like (PL), on the other hand, particles with $Y_{c.m} < 0$, constitute target like (TL) particles. In this study, v_2 for whole range of rapidity has been extracted.

In fig.4.3, the final state elliptic flow is displayed for free particles (upper panel), light charged particles (LCP's) $[2 \le A \le 4]$(middle), and intermediate mass fragments (IMF's) $[5 \le A \le A_{tot}/6]$(lower panel) at scaled impact parameter $\hat{b}$ =0.39 as a function of transverse momentum (P_t). One can see from the figure, that elliptic flow of nucleons/LCP's/IMF's is positive in the whole range of P_t. As mentioned earlier, the positive value of v_2 signifies an in-plane emission.

It is also evident from the figure that peaks of Gaussian shifts towards lower value of P_t for heavier fragments. In the intermediate energy domain, collective rotation is one of the main mechanism responsible for the positive elliptic flow. A strong pressure is built during the early stage of the reaction will transform into azimuthal aniotropy in momentum space.

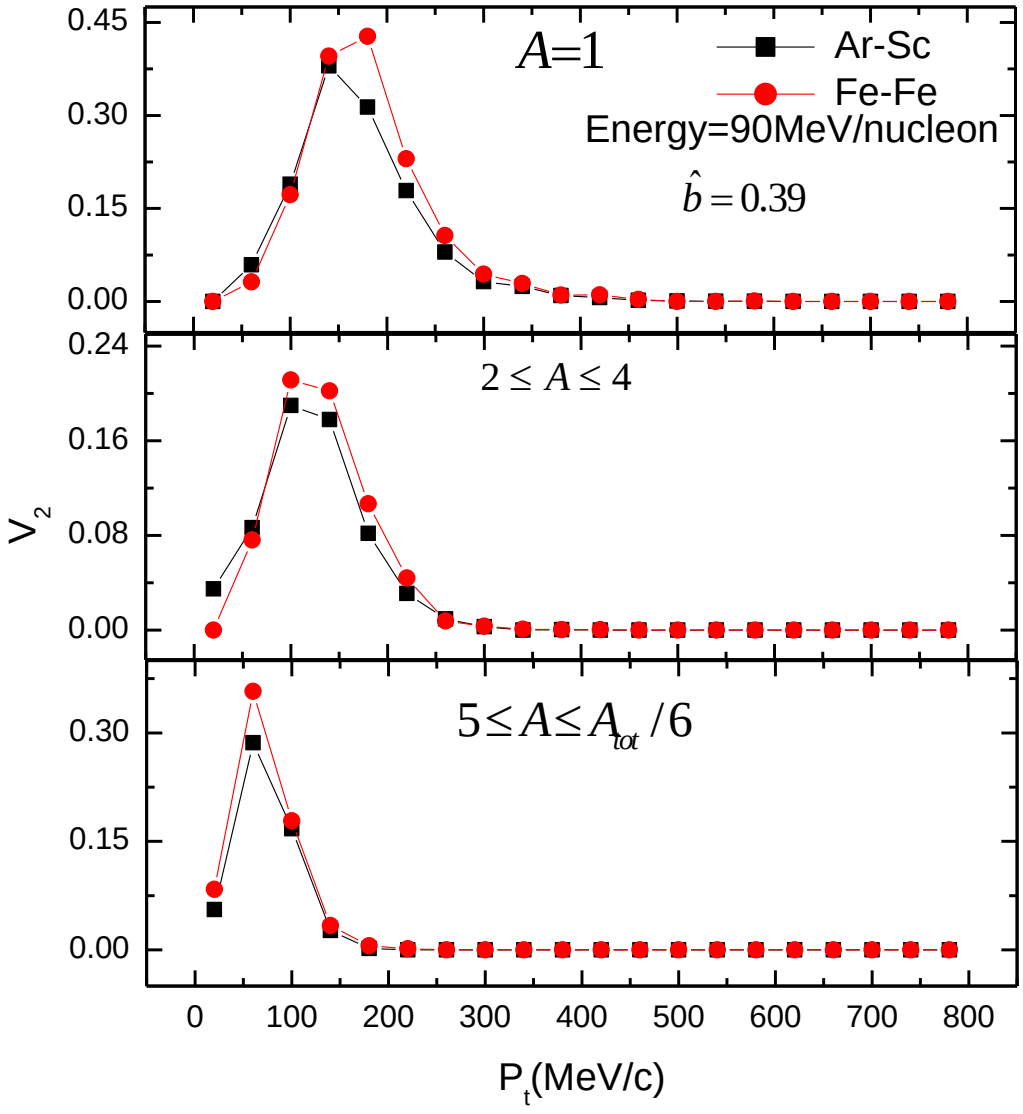

Figure 4.3: Transverse momentum dependence of elliptic flow v_2 at $\hat{b}$ = 0.39 for different symmetric reactions at 90 MeV/nucleon. The top, middle and bottom panels are representing free particles, LCP's and IMF's respectively.

In other words, elliptical flow is mainly driven by the stronger outward pressure built during the reaction. Interestingly, elliptic flow depends strongly on the isospin content of the

reaction. We note that the peak value of v_2 for free nucleons at 90 MeV/nucleon is 0.42 and 0.38 for ${}^{58}_{26}Fe+{}^{58}_{26}Fe$ and ${}^{40}_{18}Ar+{}^{45}_{21}Sc$ respectively. The mass ratio of these reactions is 1.36 and 1, whereas, N/Z ratio is 1.23 and 1.17. Here one reaction is symmetric and other is antisymmetric.

In fig.4.4, we display the variation of v_2 with beam energy for free, LCP's and IMF's. Free particles have always positive elliptical flow indicating ellipse like distribution. A sharp change is visible for lower incident energies that saturates for higher incident energies. In other words, elliptical shape of nuclear flow dominates the physics at lower energies. With the increase in the incident energy, this flow is superseded by the collective transverse flow. It is also observed that the flow of heavier fragments is larger compared to LCP's/free nucleons at all beams energies. The trend of elliptical flow in IMF's is different compared to that obtained for free nucleons/LCP's. The primary cause of this difference is the different origin of free nucleons, LCP's and IMF's. Free nucleons and LCP's are formed due to compressed zone, whereas, IMF's are the remnant of the target and projectile. In earlier studies [13,14],the transition of elliptic flow from in-plane to out-of-plane is reported at midrapidities, however, this elliptic flow transition seems to disappear, once entire rapidity range is considered.

The investigation of elliptical flow at different impact parameters is displayed in figure 4.5. Here the top, middle and bottom panels represent the free nucleons, LCP's and IMF's. The value of elliptic flow v_2 increases with the impact parameter.The complete stopping takes place at $\hat{b} = 0$, leading to zero value of elliptical flow. One can see that as we move away from central collisions, the elliptical flow increases for free and LCP's, but start saturating beyond $\hat{b} = 0.45$ for IMF's. This is because at peripheral collisions, the majot part of the colliding nuclei doesnot suffer any collision and hence there is no transverse flow production. The elliptical flow is stronger for heavy fragments compared to lighter colliding nuclei

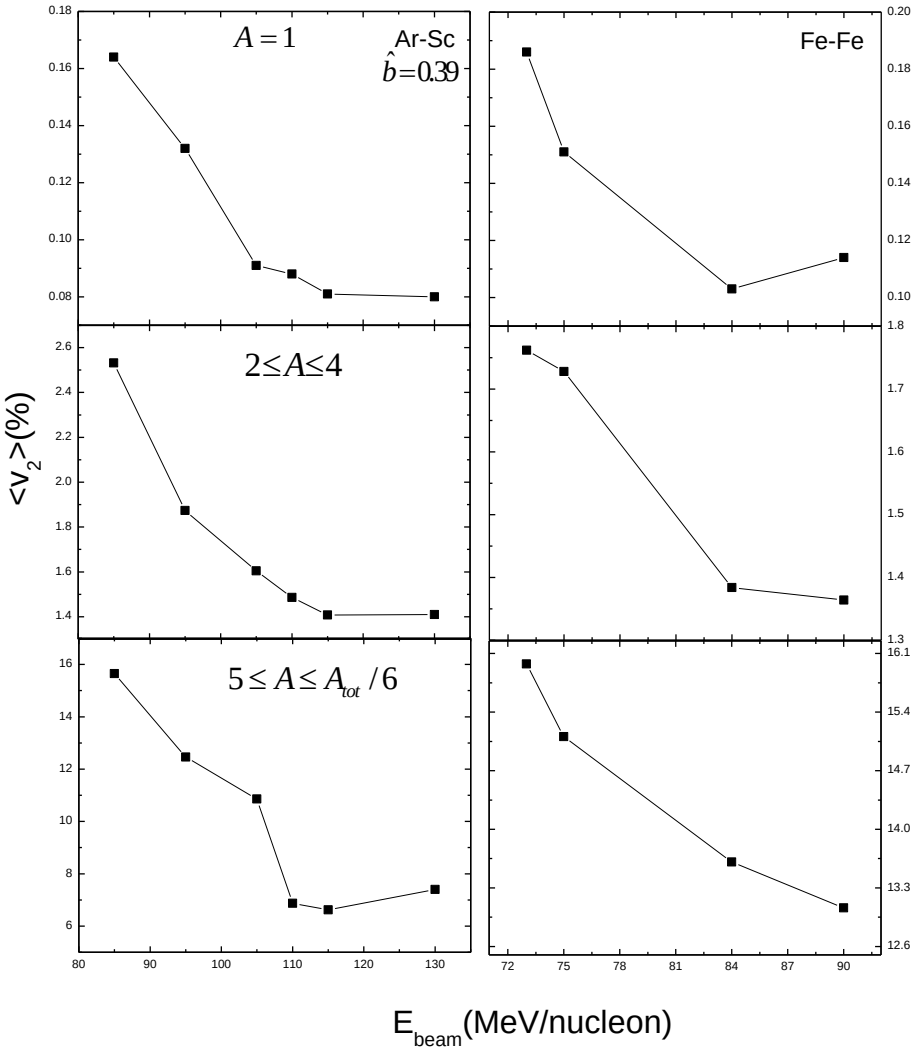

Figure 4.4: Variation of elliptic flow with beam energy at $\hat{b}$ = 0.39 for ${}^{40}_{18}Ar+{}^{45}_{21}Sc$ and ${}^{58}_{26}Fe+{}^{58}_{26}Fe$ reactions. The top, middle and bottom panels have same meaning as that of fig. 4.3.

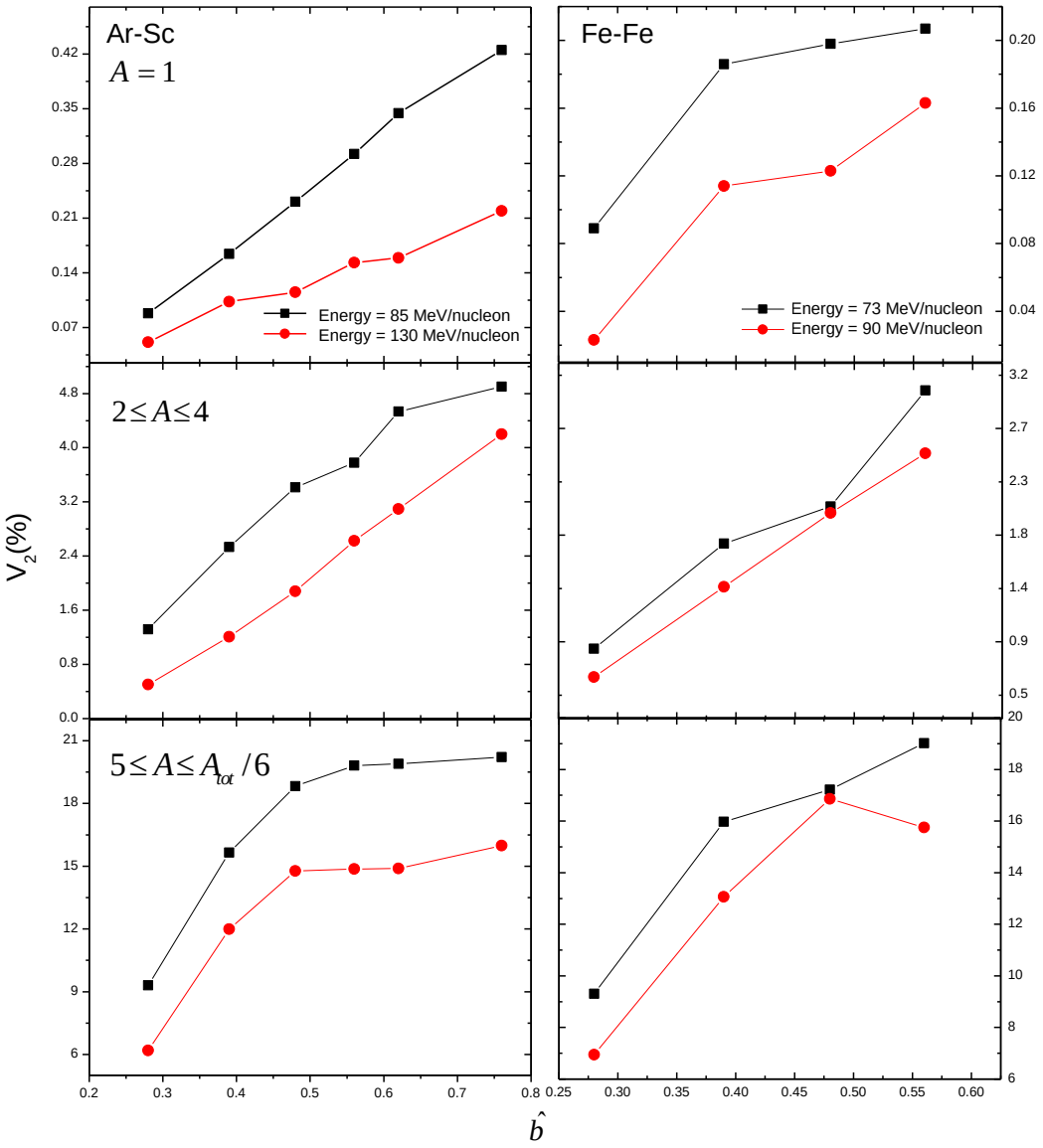

Figure 4.5: Impact parameter dependence of elliptic flow v_2 at 95 and 130 MeV/nucleon for ${}^{40}_{18}Ar+{}^{45}_{21}Sc$ and at 75 and 90 MeV/nucleon for ${}^{58}_{26}Fe+{}^{58}_{26}Fe$. The top, middle and bottom panels are for free particles, LCP's and IMF's respectively.

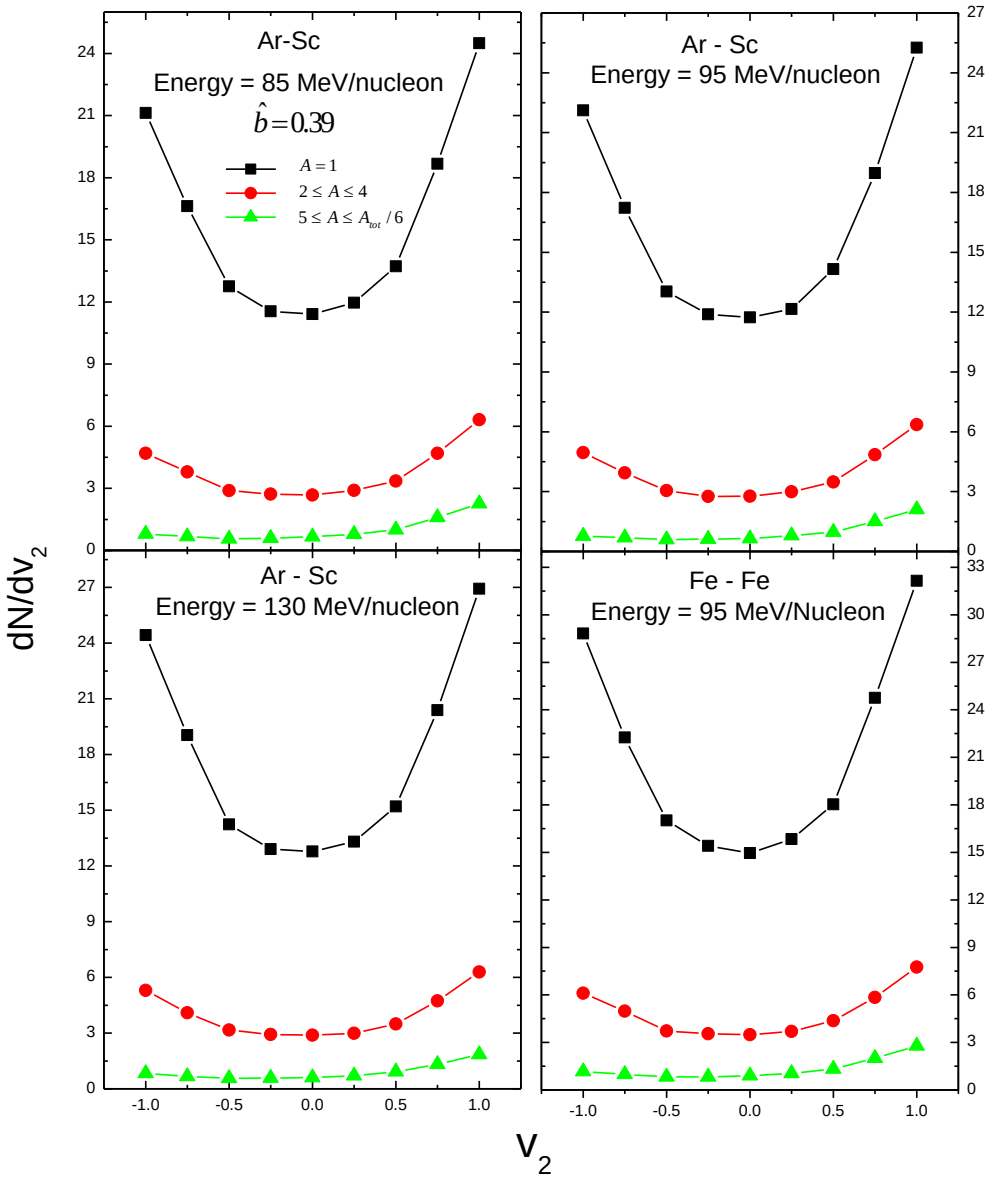

Figure 4.6: Left panel shows the distribution of free, LCP's and IMF's as a function of elliptic flow for ${}^{40}_{18}Ar+{}^{45}_{21}Sc$ at different beam energies. Right panel shows the variation with different systems (${}^{40}_{18}Ar+{}^{45}_{21}Sc$ and ${}^{58}_{26}Fe+{}^{58}_{26}Fe$) at same beam energy.

The variation of $\frac{dN}{dv_2}$ as a function of elliptic flow parameter v_2 is displayed for free, LCP's and intermediate mass fragments in fig. 4.6. The left panel is at 85 and 130 MeV for ${}^{40}_{18}Ar+{}^{45}_{21}Sc$ at $\hat{b} = 0.39$. The number of particles in a certain v_2 range goes on increasing with the beam energy and decreases with decrease in size of fragment. The right panel shows the number of particles in elliptic flow for ${}^{40}_{18}Ar+{}^{45}_{21}Sc$ and ${}^{58}_{26}Fe+{}^{58}_{26}Fe$ at beam energy of 95 MeV/nucleon. The distribution of number of nucleon in different bins of v_2 depends directly on mass of colliding nuclie. The variation of $\frac{dN}{dv_2}$ shows helical shape on on increasing the charge asymmetry i.e. when one goes from ${}^{40}_{18}Ar+{}^{45}_{21}Sc$ (N/Z = 1.17) to ${}^{58}_{26}Fe+{}^{58}_{26}Fe$ (N/Z = 1.23).

4.5 References:

[1] P. Danielewiez and G. Odyniee, Phys. Lett. B 157, 146 (1985).

[2] Q. B. Pan and P. Danielewiez, Phys. Rev. Lett. 70, 2062 (1993).

[3] J. Zhang, S. Das Gupta and C. Gale, Phys. Rev. C 50, 1617 (1994).

[4] B.A. Li, Phys. Lett. B 300, 14 (1993); Nucl. Phys. A 570, 797 (1994).

[5] J. Ollitraullt, Phys. Rev. D 46, 229 (1992).

[6] S. Voloshin, Y. Zhang, Z.Phys. C 70, 665 (1996).

[7] H. Sorge, Phys. Lett. B 402, 251 (1997).

[8] D. Teaney and E.V. Shuryak, Phys. Rev. Lett. 83, 4951 (1999).

[9] P. F. Kolb, J. Sollfrank, and U. Heinz, Phys. Rev. C 62, 054909 (2000).

[10] E. Lehmann *et.al*., Prog. Part. Nucl. Phus. 30, 219 (1993).

[11] J. Aichelin, Phys. Rep. 202, 233 (1991).

[12] J. Singh and R. K. Puri, Phys. Rev. C 62, 050602 (2000).

[13] J. Lukasik, G. Auger and M.L. Begemann-Blaich *et al*., Phys. Lett. B608, 233 (2005).

[14] Y.Zhang and Z.Li, Phys. Rev. C 74, 014601 (2006).

CHAPTER – 5

SUMMARY

This thesis contains a theoretical study of elliptical flow in heavy ion nuclear reactions. The IQMD model is used to study the elliptical flow for projectile and target of ${}^{40}_{18}Ar+{}^{45}_{21}Sc$ at E = 85, 95, 105, 110, 115 MeV/nucleon and scaled impact parameter $\hat{b}$ = 0.28, 0.39, 0.48, 0.56, 0.62, 0.76 and ${}^{58}_{26}Fe+{}^{58}_{26}Fe$ at E = 73, 75, 84, 90 MeV/nucleon and scaled impact parameter $\hat{b}$ = 0.28, 0.39, 0.48, 0.56. The details of different theoretical models was discussed in Chap. 2. We discussed in particular,isospin quantum molecular dynamics model used for present study.

In chapter 3, the time evolution of ${}^{58}_{26}Fe+{}^{58}_{26}Fe$ collisions in coordinate and momentum space respectively. Through this study, we analysed the processes involved in non-central heavy ion collisions which include the formation of initial phase, high density phase, expansion and freeze-out. The evolution of mean density and the rate of nucleon-nucleon collisions as a function of time was also done.

In chapter 4, we have attempted to understand the nature of elliptic flow in ${}^{40}_{18}Ar+{}^{45}_{21}Sc$ and ${}^{58}_{26}Fe+{}^{58}_{26}Fe$ systems at wide range of energies and impact parameters. The isospin dependence of elliptical flow is clearly visible. Transverse momentum dependence of elliptical flow is also studied. A negative value of v_2 shows the property of squeeze out effect perpendicular to reaction plane. Zero value of v_2 corresponds to isotropic distribution in transverse plane. It is observed that elliptical shape of nuclear flow dominates the physics at low and intermediate energies. With increase in energy, this flow is superseded by the collective transverse flow. The transition of elliptical flow from in-plane to out-of-plane is

reported at mid-rapidities. The value of elliptical flow increases with the impact parameter. Also the number of particles in a certain v_2 range goes on increasing with the beam energy and decreases with the increase in the size of fragment.